© 2015. Published by The Company of Biologists Ltd | Journal of Cell Science (2015) 128, 3744-3756 doi:10.1242/jcs.172536

RESEARCH ARTICLE

Failure of lysosome clustering and positioning in the juxtanuclear region in cells deficient in rapsyn

Mohamed Aittaleb[1], Po-Ju Chen[1] and Mohammed Akaaboune[1,2,*]

ABSTRACT

Rapsyn, a scaffold protein, is required for the clustering of acetylcholine receptors (AChRs) at contacts between motor neurons and differentiating muscle cells. Rapsyn is also expressed in cells that do not express AChRs. However, its function in these cells remains unknown. Here, we show that rapsyn plays an AChR-independent role in organizing the distribution and mobility of lysosomes. In cells devoid of AChRs, rapsyn selectively induces the clustering of lysosomes at high density in the juxtanuclear region without affecting the distribution of other intracellular organelles. However, when the same cells overexpress AChRs, rapsyn is recruited away from lysosomes to colocalize with AChR clusters on the cell surface. In rapsyn-deficient (*Rapsn*$^{-/-}$) myoblasts or cells overexpressing rapsyn mutants, lysosomes are scattered within the cell and highly dynamic. The increased mobility of lysosomes in *Rapsn*$^{-/-}$ cells is associated with a significant increase in lysosomal exocytosis, as evidenced by increased release of lysosomal enzymes and plasma membrane damage when cells were challenged with the bacterial pore-forming toxin streptolysin-O. These findings uncover a new link between rapsyn, lysosome positioning, exocytosis and plasma membrane integrity.

KEY WORDS: Lysosomes, Rapsyn, Clustering, Exocytosis, Mobility

INTRODUCTION

Rapsyn, a 43-kDa scaffold protein, is clustered on postsynaptic membranes of the Torpedo electric organ and vertebrate neuromuscular junctions (NMJs) where it tightly colocalizes with nicotinic acetylcholine receptors (AChRs) at the top of the junctional folds (Noakes et al., 1993; Sanes and Lichtman, 1999). Rapsyn is best known for its role in clustering and maintaining a high density and number of AChR at synaptic sites (Froehner et al., 1981; Noakes et al., 1993; Gautam et al., 1995). For instance, in mice deficient in rapsyn, AChRs and other specific synaptic proteins fail to cluster on the muscle postsynaptic domain and mice die immediately after birth. In addition, at mature NMJs short hairpin RNA (shRNA)-mediated knockdown of rapsyn induces the disassembly of existing AChR clusters (Kong et al., 2004; Martínez-Martínez et al., 2009). In human neuromuscular synapses, rapsyn mutations cause a decrease in AChR levels at the synapse, leading to severe myasthenic syndrome (Ohno et al., 2002; Maselli et al., 2003). Rapsyn has also been found to interact with β-dystroglycan, and the β-catenin–α-catenin complex (Zhang et al., 2007), linking AChRs to cytoskeletal components (Moransard et al., 2003). Rapsyn has also been found in non-muscle cell types and undifferentiated myoblasts (Frail et al., 1989; Musil et al., 1989). However, neither the physiological function nor the localization of rapsyn in these cells has been studied.

Structural and functional studies have revealed that rapsyn contains a myristoylation site necessary for sub-membrane localization, seven tetratricopeptide repeats (TPRs) required for self-association, a putative coiled-coil domain essential for interaction with AChRs and a cysteine-rich RING-H2 domain required for interaction with β-dystroglycan, a component of the dystrophin glycoprotein complex that is linked to the actin cytoskeleton network (Carr et al., 1989; Phillips et al., 1991; Ramarao and Cohen, 1998; Bartoli et al., 2001; Ramarao et al., 2001). However, it remains unknown the role of these rapsyn structural features, most notably, the myristoylation, coiled-coil and RING domains, is in the clustering and positioning of intracellular organelles such as lysosomes. Increasing evidence suggests that lysosomal positioning plays an important role in coordinating cellular responses during nutrient starvation (Korolchuk et al., 2011). It has also been shown that lysosomal exocytosis plays an essential role in the resealing of the plasma membrane after damage (Miyake and McNeil, 1995; Reddy et al., 2001; Chakrabarti et al., 2003; Andrews et al., 2014). Here, we sought to examine whether rapsyn can be a key regulatory component of the dynamic state of lysosomes, notably lysosomal exocytosis.

To address these issues, we used gain- and loss-of-function approaches and live-cell imaging microscopy. We found that rapsyn is colocalized with lysosomes and selectively concentrates at junctional sites between lysosomes. Mutation of the myristoylation site or deletion of either the coiled-coil or RING-H2 domain prevented the targeting of rapsyn to lysosomes. In rapsyn-deficient myoblasts, lysosomes failed to cluster, leading to their scattering throughout the entire cytoplasm, a defect that was rescued by wild-type but none of mutated forms of rapsyn. Finally, we showed that rapsyn controls lysosome exocytosis, as the release of lysosomal enzymes was significantly increased in rapsyn-deficient cells. Taken together, these results suggest that rapsyn controls the positioning of lysosomes, which might play an important role in the resealing of the plasma membrane.

RESULTS

Rapsyn specifically localizes to lysosomes

It is well-established that rapsyn plays a crucial role in the clustering of acetylcholine receptors (AChRs) on the surface of muscle cells (Gautam et al., 1995; Sanes and Lichtman, 2001). Because rapsyn is also expressed in cells that never produce AChRs, we asked whether rapsyn had any function in the absence of AChRs. To address this issue, we first surveyed the expression of rapsyn in non-muscle cells and undifferentiated myoblast cells. Lysates from various cells (COS-7, PC12, HEK293, NIH3T3 and CHO) and undifferentiated C2C12 myoblasts were probed by western blotting with a rabbit monoclonal anti-rapsyn antibody. We detected rapsyn in each of

[1]Department of Molecular, Cellular, and Developmental Biology, University of Michigan, Ann Arbor, MI 48109, USA. [2]Program in Neuroscience, University of Michigan, Ann Arbor, MI 48109, USA.

*Author for correspondence (makaabou@umich.edu)

Received 31 March 2015; Accepted 23 August 2015

Journal of Cell Science (2015) 128, 3744-3756 doi:10.1242/jcs.172536

these lysates (Fig. 1A), consistent with previous reports that also detected rapsyn in undifferentiated C2C12 myoblasts (Frail et al., 1989) and non-muscle cells (Musil et al., 1989). Next, we examined the intracellular localization of rapsyn. Undifferentiated myoblasts were co-transfected with rapsyn–EGFP and Lamp1–mCherry (a marker of lysosomes; Chen et al., 1985, 1986), mCherry–EEA1 (a marker of early endosomes; Stenmark et al., 1996), ManII–mCherry (a marker of Golgi; Zilberman et al., 2011) or mCherry-PDiA (a marker of endoplasmic reticulum; Mouslim et al., 2012). We found that rapsyn–EGFP colocalized perfectly with Lamp1–mCherry in the juxtanuclear region of undifferentiated C2C12 myoblasts, but not with mCherry–EEA1, ManII–mCherry (Fig. 1B) or mCherry–PDiA (Fig. S1A). Similar colocalization of rapsyn–EGFP with Lamp1–mCherry was also observed in non-muscle cells (COS, PC12 and NIH3T3) (Fig. S1B). Taken together, these results indicate that rapsyn is specifically localized to lysosomes. In a second set of experiments, cells were transfected with rapsyn–EGFP, fixed and immunostained with antibodies against intracellular organelle markers (Lamp1 for lysosomes, EEA1 for endosomes or GM130 for the Golgi). Similar to results obtained using overexpressed markers, rapsyn–EGFP was found to overlap specifically with the lysosomal marker Lamp1 but not with the other markers (Fig. 1C). These results suggest that overexpression of the Lamp1–mCherry construct has no effect on lysosome distribution in transfected cells. In light of these results, we used the Lamp1–mCherry construct as a tool for the identification of lysosomes in subsequent experiments.

To gauge the lysosomal localization of rapsyn with better resolution, we took advantage of the availability of vacuolin-1, a small molecule that has been shown to promote the formation of enlarged vacuoles derived from the fusion of endosomes and lysosomes (Huynh and Andrews, 2005). C2C12 myoblasts or COS-7 cells were co-transfected with rapsyn–EGFP and Lamp1–mCherry, treated with vacuolin-1 for ∼3 h, and cells expressing both constructs were then imaged live with a spinning disk confocal microscope. Remarkably, rapsyn was concentrated specifically at the junctions between vacuoles in both undifferentiated myoblasts (Fig. 2A) and COS-7 cells (Fig. 2B).

It is possible that rapsyn–EGFP is targeted to lysosomes for degradation. If so, then the absence of rapsyn–EGFP inside lysosomal vacuoles could be due to the quenching of GFP fluorescence by the acidic environment of the lumen. To rule out this possibility, we generated a rapsyn–mCherry construct, as mCherry is known to resist quenching by acidic pHs and remains fluorescent in an acidic environment (Shaner et al., 2004). If rapsyn was digested by lysosomes, overexpressed rapsyn–mCherry would accumulate inside lysosomes during the degradation process and rapsyn degradation products would be detected with western blotting. However, when cells were transfected with rapsyn–mCherry, similar to rapsyn–EGFP localization, rapsyn was localized to junctional sites between lysosomes with no apparent fluorescence in the lumen (Fig. S1C), and no rapsyn degradation products were seen when western blotting was performed on cells transfected with rapsyn–EGFP (Fig. S1D). These results indicate

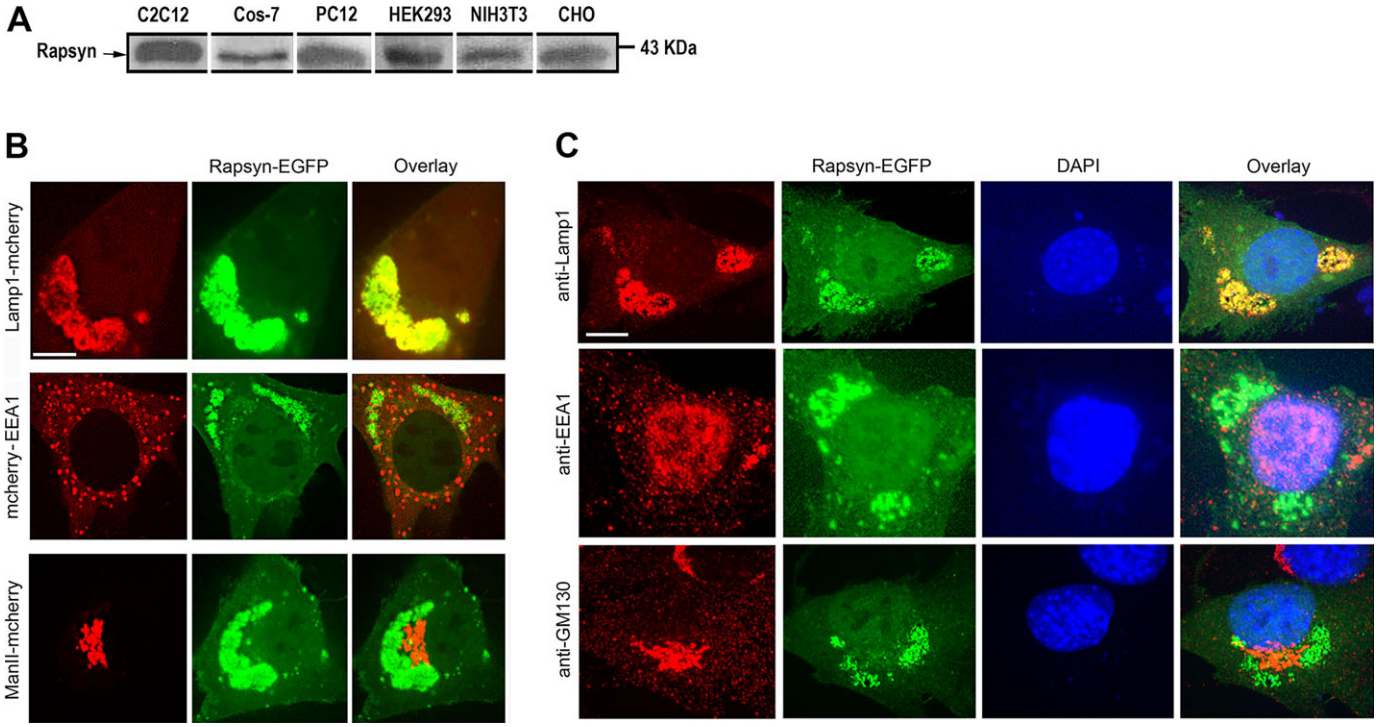

Fig. 1. Rapsyn expression and localization in non-muscle and undifferentiated myoblast cells. (A) Immunoblots of lysates from undifferentiated C2C12 myoblasts and non-muscle cell types (COS-7, PC12, HEK293, NIH3T3 and CHO) probed with rabbit monoclonal anti-rapsyn antibody. Note that rapsyn is present in extracts of all examined cells. (B) Undifferentiated C2C12 myoblasts were co-transfected with rapsyn–EGFP and either the lysosomal marker Lamp1–mCherry, early endosome marker mCherry–EEA1 or Golgi marker ManII–mCherry and then cells expressing fluorescent fusion proteins were live imaged using the confocal spinning disk microscope. In the top left panel representative images of live C2C12 myoblasts co-transfected with rapsyn–EGFP and lysosomal marker Lamp1–mCherry are shown; in the middle left panel rapsyn–EGFP and early endosome marker mCherry–EEA1 are shown; in the bottom left panel rapsyn–EGFP and Golgi marker ManII–mCherry are shown. Note that rapsyn colocalizes only with lysosomes. (C) Immunostaining of C2C12 myoblasts expressing rapsyn–EGFP with rat anti-Lamp1, rabbit anti-EEA1 or mouse anti-GM130 antibodies. Note that rapsyn localizes to lysosomes but not to endosomes or Golgi. Scale bars: 10 µm.

Journal of Cell Science (2015) 128, 3744-3756 doi:10.1242/jcs.172536

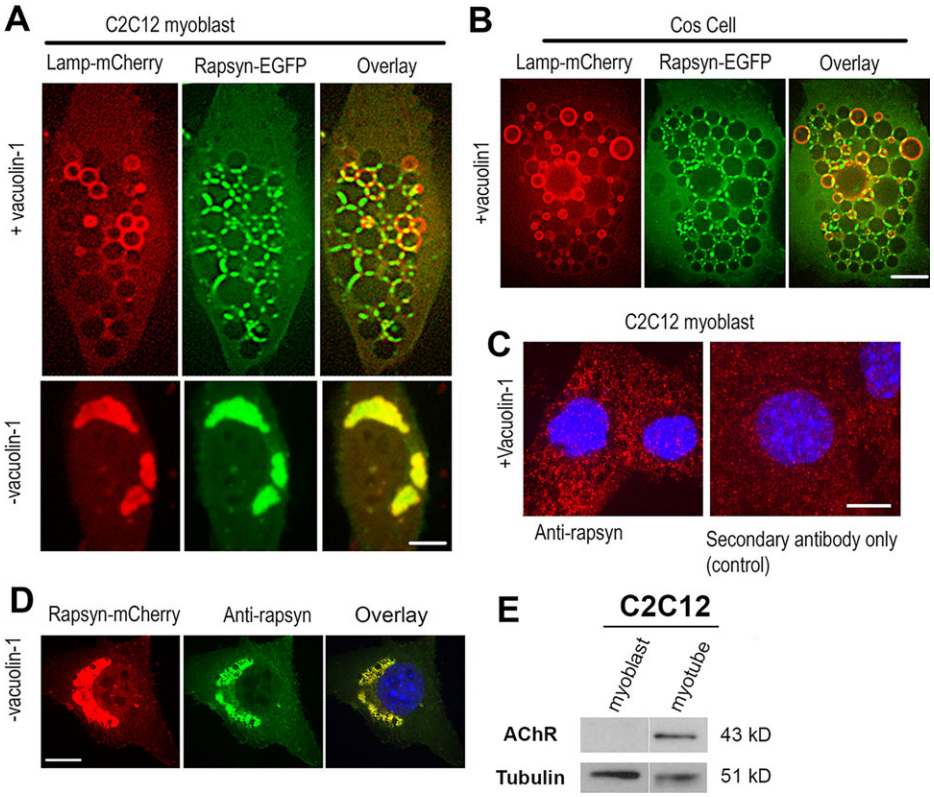

Fig. 2. Rapsyn concentrates at junctional sites between vacuolin-1 enlarged lysosomal vacuoles. (A) Undifferentiated C2C12 myoblasts or (B) non-muscle COS-7 cells were transfected with rapsyn–EGFP and Lamp1–mCherry and either left untreated (lower panels) or treated with vacuolin-1 (upper panels). Rapsyn–EGFP colocalizes perfectly with Lamp1–mCherry in the juxtanuclear region of non-treated C2C12 myoblasts (A, lower panels) and is concentrated at the junctional sites between enlarged lysosomal vacuoles visualized by Lamp1–mCherry (A, upper panels) and in COS cells (B). (C) C2C12 myoblasts were treated with vacuolin-1, fixed and labeled with mouse monoclonal anti-rapsyn antibody followed by a secondary fluorescent antibody (left panel) or with a fluorescent secondary antibody only (right panel). (D) C2C12 myoblast transfected with rapsyn–mCherry, fixed and labeled with antibody against rapsyn. Scale bars: 10 µm. (E) Blot showing that AChRs are undetectable in undifferentiated myoblasts.

that targeting of rapsyn to lysosomes does not lead to its degradation. To determine whether endogenous rapsyn also localizes to lysosomes, C2C12 myoblast cells were fixed and immunostained with antibody against rapsyn. In untreated cells with vacuolin-1, rapsyn could not be detected (presumably due to low concentration of endogenous rapsyn at lysosomes despite its presence in high concentration in cell lysates). However, when myoblast cells were treated with vacuolin-1 (so endogenous rapsyn can be concentrated at junctions between lysosomal vacuoles) and immunostained, the endogenous expression of rapsyn was found to be concentrated at the junctional sites between lysosomal vacuoles (the staining intensity is above background fluorescence compared to staining with secondary antibody alone) (Fig. 2C). As a positive control for rapsyn antibody, rapsyn–mCherry in myoblasts was also immunostained (Fig. 2D). Of note, in non-differentiated myoblasts at ~80% confluence, AChR expression was undetectable (Fig. 2E).

Next, we tested whether other postsynaptic proteins that form complex with rapsyn and/or cluster with AChRs at synapses (α-dystrobrevin, α-syntrophin or muscle-specific isoform CamKIIβ) are also concentrated at lysosome junctions. To do this, myoblasts were co-transfected with Lamp1–mCherry and GFP fusions of either α-dystrobrevin, α-syntrophin or the muscle-specific Ca^{2+}/calmodulin-dependent protein kinase II isoform CamKIIβ and then treated with vacuolin-1. We found that none of these postsynaptic proteins was concentrated at the junctional space between lysosomes, but instead all were diffusely distributed throughout the cytosol (Fig. 3), suggesting that the localization to junctional sites between vacuoles is specific and selective for rapsyn.

Next, we asked whether the targeting of rapsyn to lysosomes is affected by the presence of AChRs. To do this, myoblast cells were co-transfected with low or high concentrations of rapsyn–EGFP and the four subunits of mouse AChR. After 24 h, myoblasts were fixed without permeablization, incubated with BTX–Alexa-Fluor-594, and then imaged with the confocal microscope. At low concentration of rapsyn–EGFP, we found that most of rapsyn was targeted with AChRs to the surface of myoblasts (Fig. 4A). In cells transfected with a high concentration of rapsyn–EGFP, rapsyn was found both concentrated at the lysosomes and clustered with AChRs receptors at the cell surface (Fig. 4A). However, when cells were transfected with rapsyn–EGFP and the lysosomal marker Lamp1, rapsyn was mainly found with lysosomes in the juxtanuclear region (Fig. 4B).

Targeting of rapsyn to lysosome junctions requires the myristoylation, coiled-coil domain and RING-H2 domain

Previous studies have shown that rapsyn has distinct structural features with different functions (Phillips et al., 1991; Ramarao et al., 2001). We sought to determine which structural features are required for targeting rapsyn to lysosome junctions. For this purpose, we designed a series of rapsyn–EGFP mutants (Fig. 5A), in which we mutated Gly2 to Ala (G2A) to abolish myristoylation (a lipid modification that anchors proteins into the lipidic membranes; Carr et al., 1989; Resh, 2004), deleted the coiled-coil domain (ΔCC) (shown to mediate interaction with AChRs; Ramarao and Cohen, 1998; Ramarao et al., 2001) or deleted the RING-H2 domain (ΔH2) (the RING-H2 domain was shown to mediate binding with α-dystroglycan; Bartoli et al., 2001). Lysates from COS cells expressing these rapsyn–EGFP mutants were first blotted with anti-GFP or anti-rapsyn antibodies, which showed the corresponding proteins at the expected sizes, confirming the production of intact protein fusions (Fig. 5B). Each of these rapsyn–EGFP constructs was co-transfected with Lamp1–mCherry into undifferentiated C2C12 myoblasts. Myoblasts were treated with vacuolin-1 24 h later, and cells expressing both Lamp1–mCherry and rapsyn–EGFP were imaged live. As shown in Fig. 5C, we found that the lack of myristoylation (G2A–EGFP) resulted in a loss of rapsyn localization to lysosomes, and instead rapsyn predominantly accumulated in the nucleus. Similarly,

Journal of Cell Science (2015) 128, 3744-3756 doi:10.1242/jcs.172536

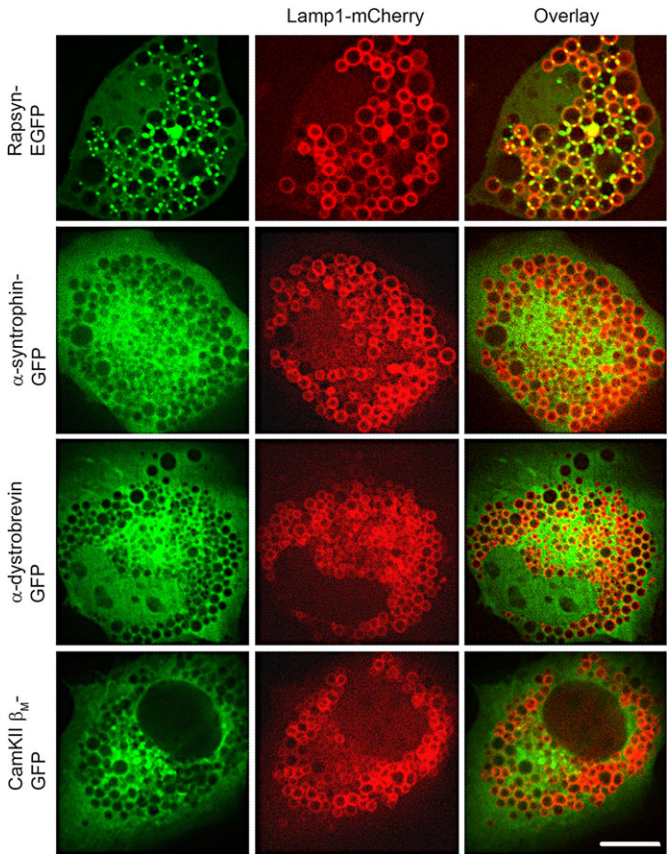

Fig. 3. Rapsyn, but not other proteins of the postsynaptic complex, is selectively targeted to lysosomes. C2C12 myoblasts were co-transfected with Lamp1–mCherry and either rapsyn–EGFP, α-syntrophin–GFP, α-dystrobrevin–GFP or CamKIIβM–GFP. Cells were then treated with vacuolin-1 prior to live imaging by confocal spinning disk microscope. Representative images showing that rapsyn–EGFP accumulates selectively at the junctional sites between enlarged lysosomal vacuoles whereas α-syntrophin–GFP, α-dystrobrevin–GFP or CamKIIβM–GFP showed a diffuse distribution throughout the cytoplasm, with no localization to the vacuoles. Scale bars: 10 µm.

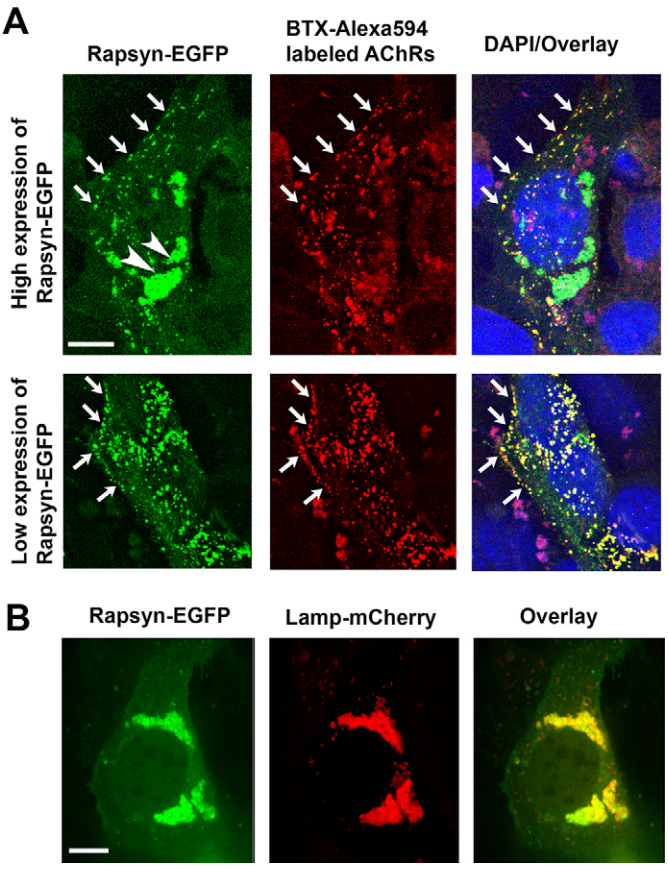

Fig. 4. Rapsyn is recruited to the cell surface in the presence of AChRs. C2C12 myoblasts were co-transfected with rapsyn–EGFP and either (A) AChRα, AChRβ, AChRδ and AChRε subunits or (B) Lamp1–mCherry. (A) In C2C12 myoblasts expressing AChRs and high levels of rapsyn–EGFP, rapsyn is concentrated in the juxtanuclear region (arrowheads) and colocalizes with AChR clusters at the cell surface (upper panel). However, in myoblast expressing AChRs and low level of rapsyn, most rapsyn molecules are recruited to AChR clusters at the cell surface (lower panel). Arrows indicate co-clusters of AChRs and rapsyn at the cell surface. (B) When myoblasts were transfected with rapsyn–EGFP and Lamp1–mCherry, rapsyn remains largely concentrated with Lamp1–mCherry in the juxtanuclear region (no visible accumulation at the cell surface). Scale bars: 10 µm.

deletion of either the coiled-coil (ΔCC–EGFP), RING-H2 (ΔRINGH2–GFP) or both (ΔCC/RINGH2–GFP) domains resulted in a loss of lysosomal localization of rapsyn and instead these rapsyn mutants displayed a diffuse distribution throughout the entire cytoplasm. These results indicate that N-terminal myristoylation, coiled-coil and RING H2 domains are required for the targeting of rapsyn to lysosomes and its concentration at their junctional sites. These results also indicate the possibility that the specific localization of rapsyn between lysosomal vacuoles was due to the self-association of rapsyn (Ramarao et al., 2001), which is unlikely since all known self-association domains remained intact in each of these mutants. Similar results were obtained in COS-7 cells (Fig. S2A).

Rapsyn induced the clustering of lysosomes in the juxtanuclear region

Given the specific colocalization of rapsyn with lysosomes, we hypothesized that rapsyn might play a role in the clustering of lysosomes. To test this idea, we first conducted gain-of-function experiments on undifferentiated myoblasts. In cultured myoblasts, lysosomes are typically distributed in the juxtanuclear region with a few additional lysosomes scattered throughout the cytoplasm (Matteoni and Kreis, 1987). However, when cells were co-transfected with Lamp1–mCherry and wild-type rapsyn–EGFP, lysosomes became more compact in the juxtanuclear region and very few lysosomes were distributed throughout the cytoplasm compared to control cells expressing Lamp1–mCherry only (Fig. 6A). Quantification showed that in cells expressing rapsyn–EGFP, lysosomes occupied only 45% (128±10 µm^2, mean±s.e.m., n=36) of the area that lysosomes occupied in control C2C12 myoblasts (284±12 µm^2, mean±s.e.m., n=55) (Fig. 6B). By contrast, the lysosomal compactness index was 2.5-fold higher in cells transfected with rapsyn–EGFP (0.15±0.01, mean±s.e.m., n=20) than in control cells (0.06±0.005, mean±s.e.m., n=51), (P<0.001) (Fig. 6C). The distribution of endosomes, however, was not affected by exogenous expression of rapsyn (see Fig. 1B) and the area that endosomes occupied in cell transfected with rapsyn (805±29 µm^2) was not significantly different from that of the non-transfected cells (877±35 µm^2).

Next, we asked whether preventing rapsyn from localizing to lysosomes affects the clustering of lysosomes. To test this, we first co-overexpressed a rapsyn–EGFP construct lacking the myristoylation site (G2A) with Lamp1–mCherry in undifferentiated myoblasts and

Journal of Cell Science

Journal of Cell Science (2015) 128, 3744-3756 doi:10.1242/jcs.172536

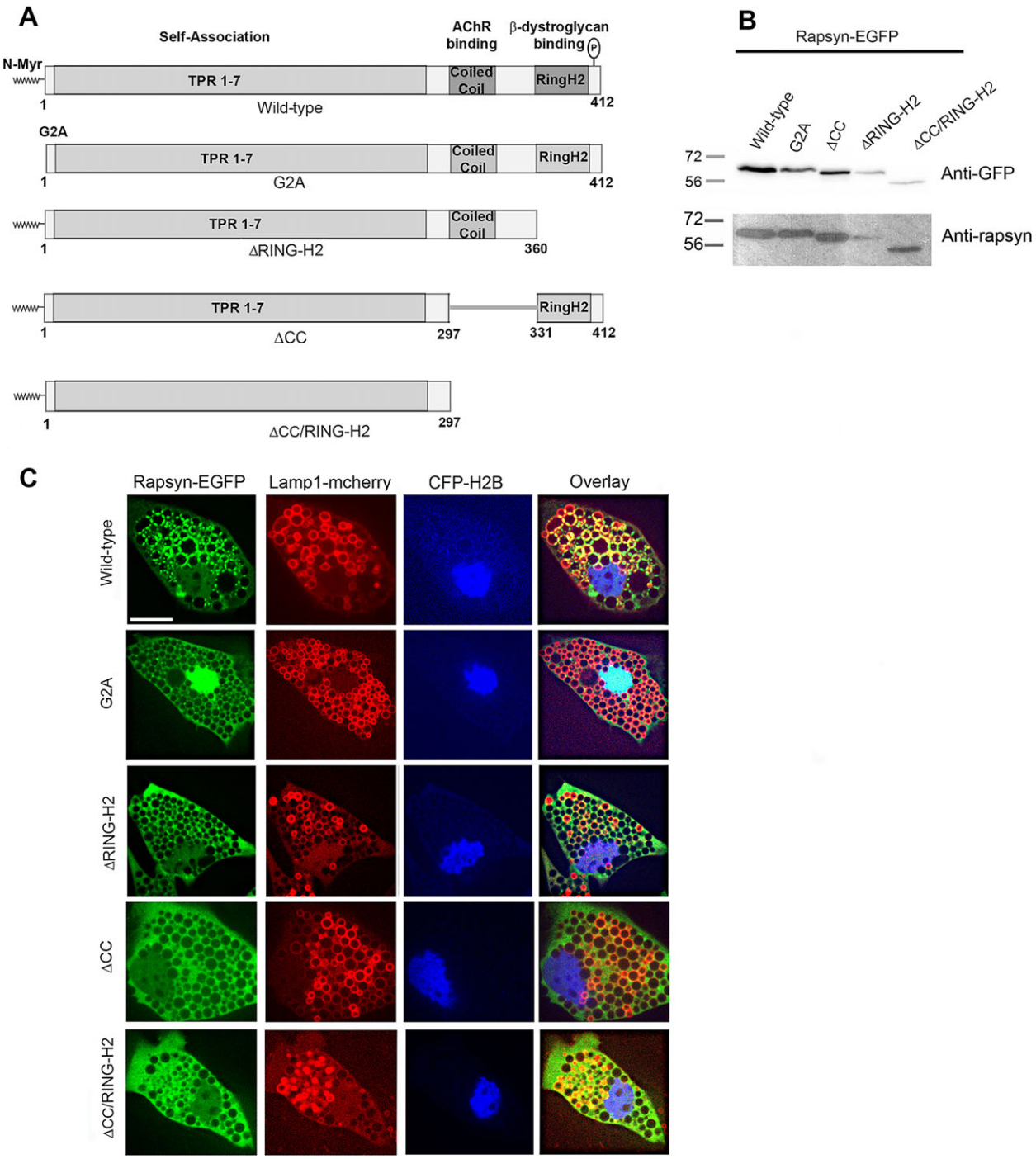

Fig. 5. The targeting of rapsyn to the junctional sites between lysosomal vacuoles requires the myristoylation, coiled-coil and RING-H2 domains. (A) Schematic representation of rapsyn constructs used as EGFP fusions in this study. (B) Lysates from COS cells expressing the indicated rapsyn–EGFP construct were blotted with anti-GFP or anti-rapsyn antibody and showed the corresponding proteins at expected sizes confirming the intact protein fusions. (C) C2C12 myoblasts were co-transfected with Lamp1–mCherry (a lysosomal marker), CFP-H2B (a nuclear marker) and either wild-type or the indicated rapsyn–EGFP mutant and then treated with vacuolin-1. Shown are representative images of cells transfected with Lamp1–mCherry and the indicated rapsyn–EGFP construct. Note that non-myristoylated rapsyn G2A–EGFP is concentrated in the nucleus. Rapsyn ΔCC–EGFP, rapsyn ΔRING-H2–EGFP and rapsyn ΔCC/RING-H2–EGFP are more diffuse in the cytoplasm whereas wild-type rapsyn–EGFP is concentrated at junctional sites between enlarged lysosomes. Scale bar: 10 μm.

analyzed the clustering of lysosomes in the cytoplasmic juxtanuclear region. In contrast to control myoblasts or myoblasts transfected with wild-type rapsyn, we found that fewer lysosomes clustered in the juxtanuclear region and that most lysosomes were scattered throughout the entire cytoplasm (Fig. 6A). Interestingly, in these cells, the area occupied by lysosomes (589±35 μm^2, mean±s.e.m., n=37) was double that of control myoblasts and ~5 times larger than wild-type rapsyn–EGFP-transfected cells (Fig. 6B). These results indicate that overexpression of the rapsynG2A–EGFP mutant induced the dispersion of the lysosomes throughout the cytosol. The compactness index of lysosomes in cells expressing rapsynG2A–EGFP (0.016±0.001, mean±s.e.m., n=17) was only 25% of the value

Journal of Cell Science (2015) 128, 3744-3756 doi:10.1242/jcs.172536

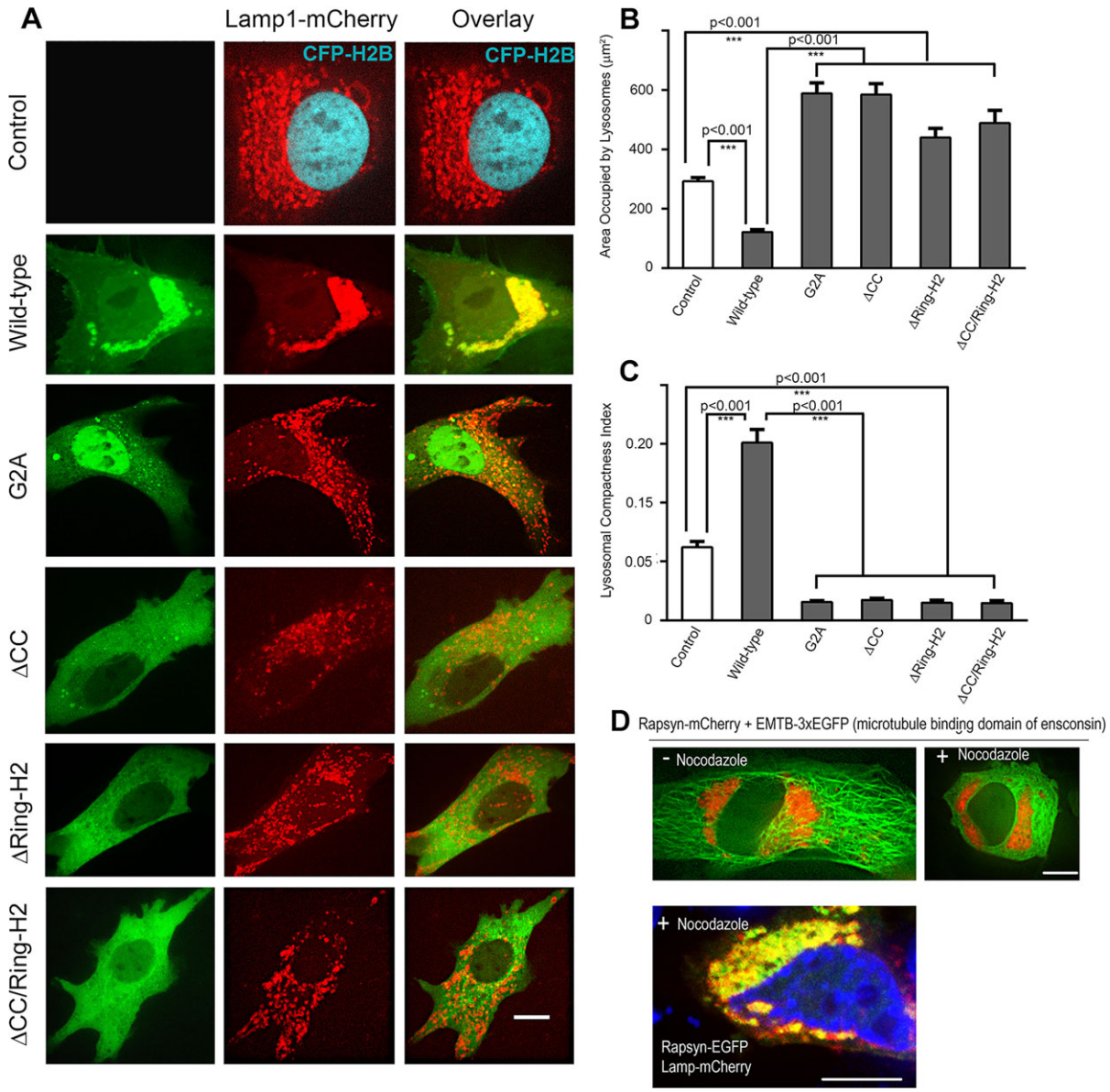

Fig. 6. Overexpression of rapsyn mutants induces the declustering of lysosomes and disruption of microtubules had no effect on rapsyn and lysosomes clusters in the juxtanuclear region. C2C12 myoblasts were transfected with Lamp1–mCherry (a lysosomal marker) and CFP–H2B to label the nuclei (control) or co-transfected with Lamp1–mCherry and either wild-type, G2A, ΔCC, ΔRING-H2 or ΔCC/RING-H2 rapsyn–EGFP constructs. CFP–H2B was only used when myoblasts were transfected with Lamp1–mCherry alone to better visualize the nucleus. Transfected myoblasts were then imaged live using confocal spinning disk microscopy. (A) Representative images of cells expressing the lysosomal marker Lamp1–mCherry and CFP–H2B (control) or Lamp1–mCherry and the indicated form of rapsyn–EGFP. Note that the clustering of lysosomes in the juxtanuclear region was significantly increased in presence of wild-type rapsyn–EGFP, whereas rapsyn mutant constructs induced the declustering of lysosomes and their scattering throughout the cytoplasm. (B) Graph showing the area occupied by lysosomes in μm^2. Note that in the presence of wild-type rapsyn, the area occupied by lysosomes is decreased compared to control cells, whereas this area is significantly increased in the presence of each rapsyn mutant. (C) Graph showing quantification of the lysosomal compactness index. Note that compactness index significantly increased in the presence of wild-type rapsyn, but dramatically decreased in the presence of rapsyn mutants compared to untransfected cells. The compactness index was determined as described in the Materials and Methods and as reported previously (Bard et al., 2003; Zilberman et al., 2011). The *P*-values were calculated using a Bonferroni test. Results are mean±s.e.m. (D) Myoblasts were transfected with rapsyn–mCherry and EMTB–3×EGFP or rapsyn–EGFP and Lamp1–mCherry and then treated with nocodazole, a drug that disrupts microtubules. Upper panels show examples of myoblast cells untreated or treated with nocodazole that were live imaged using a confocal spinning disk. The lower panel shows an example of a myoblast that was treated with nocodazole, fixed and imaged. Note that in the presence of nocodazole, rapsyn and lysosomes clusters remained intact in the juxtanuclear region whereas the microtubule-binding domain of ensconsin–EGFP was completely disrupted. Scale bars: 10 μm.

in control cells and ~10% of the value in cells expressing wild-type rapsyn–EGFP ($P<0.001$) (Fig. 6C). This suggests that overexpression of rapsyn lacking the myristoylation site is able to induce the declustering of lysosomes and that myristoylation of the N-terminal glycine is required not only for targeting rapsyn to lysosomes, but also for the juxtanuclear clustering of lysosomes (Fig. 6A–C). Thus, it appears that rapsyn lacking myristoylation acts as a dominant negative, inducing the declustering of lysosomes.

Similarly, in cells transfected with rapsyn lacking the coiled-coil or RING-H2 domain, the juxtanuclear distribution of lysosomes was also impaired, with more lysosomes scattered into a larger area of the cytoplasm (Fig. 6A). The area occupied by lysosomes in cells

Journal of Cell Science (2015) 128, 3744-3756 doi:10.1242/jcs.172536

expressing rapsynΔCC–EGFP was 585±37 μm^2 (mean±s.e.m., n=37) and in cells expressing rapsynΔH2–EGFP this area was 440±30 μm^2 (mean±s.e.m., n=17), about 4.5- and 3.4-fold greater than in the presence of wild-type rapsyn–EGFP, respectively (Fig. 6B). Similar to the rapsyn-G2A mutant, the compactness index of lysosomes in cells expressing rapsynΔCC–EGFP (0.017±0.001, mean±s.e.m., n=18) or rapsynΔH2–EGFP (0.015±0.002, mean±s.e.m., n=10) was ∼29% and 25% of that of control cells, respectively (P<0.001) and about 12% and 10% of that of cells expressing wild-type rapsyn-EGFP, respectively (Fig. 6C). When both coiled-coil and RING-H2 domains were deleted from rapsyn, no additive effect on the declustering of lysosomes was observed (Fig. 6A–C). Taken together, these results indicate a role of rapsyn in the maintenance of the lysosome clusters in the juxtanuclear region.

Previous studies have shown that several factors including microtubules control lysosomal localization in the perinuclear region (Granger et al., 2014). Here, we wanted to know whether the effect of overexpression of rapsyn on lysosomal localization and clustering could be impaired by disrupting microtubules. To do this C2C12 myoblasts were either cotransfected with rapsyn–mCherry and the microtubule-binding domain of ensconsin (EMTB) fused to three EGFP (3×EGFP) molecules (to visualize microtubules) (Miller and Bement, 2009), or co-transfected with rapsyn–EGFP and Lamp1–mCherry and then treated with nocodazole, a drug that disrupts microtubules (10 μg/ml for 90 min). Surprisingly, we found that in the presence of nocodazole (the efficiency of nocodazole treatment was assessed by disruption of EMTB–3×EGFP), there was no significant dispersion of lysosomal or rapsyn–EGFP clusters compared to untreated myoblasts (Fig. 6D). This result suggests that the ‘stickiness’ of lysosomes to rapsyn in the perinuclear region remains unaffected by disruption of the microtubules at least on the time scale of our experiment.

Lysosomes are highly mobile in cells overexpressing rapsyn mutants

Prompted by the finding that rapsyn mutants appeared to induce the dispersion of lysosomes, we examined whether the mobility of lysosomes is also affected. Using time-lapse imaging, the movement of individual lysosomes was monitored in cells expressing Lamp1–mCherry alone (control) or coexpressing Lamp1–mCherry and either wild-type rapsyn–EGFP or the rapsyn G2A–EGFP mutant. For co-transfected preparations, we analyzed only cells that showed high expression of rapsyn–EGFP. In cells transfected with the rapsynG2A–EGFP mutant, lysosomes had a mean velocity of 0.097 μm/s (Movie 2) compared to control cells in which lysosomes have a mean velocity of 0.05 μm/s (Movie 1). In contrast, in cells transfected with wild-type rapsyn–EGFP the mobility of lysosomes was restricted to the juxtanuclear region and was significantly reduced if not completely abolished (mean velocity is 0.001 μm/s, in many cases it was immeasurable, see Movie 3). These results indicate that in the absence of overexpressed rapsyn, lysosomes are highly mobile and suggest that rapsyn is required for their accumulation in the juxtanuclear region.

Juxtanuclear clustering of lysosomes is abolished in rapsyn-deficient myoblasts

To further investigate the role of rapsyn in the clustering of lysosomes, we used muscle cells derived from mutant mice that are deficient in rapsyn (*Rapsn*$^{-/-}$; clone 11-7) (Fuhrer et al., 1999). The absence of endogenous expression of rapsyn was confirmed by probing lysates from rapsyn-deficient myoblasts by western blotting with anti-rapsyn antibody (Fig. 7A). To examine the effect of the absence of rapsyn on the clustering of lysosomes, rapsyn-deficient myoblasts were transfected with Lamp1–mCherry and cells were imaged live with a spinning disk confocal microscope. Unlike in C2C12 and *Rapsn*$^{+/+}$ myoblasts, lysosomes in *Rapsn*$^{-/-}$ myoblasts were not clustered at the cytoplasmic juxtanuclear region but were instead scattered throughout the entire cytoplasm (Fig. 7B). However, the distribution of early endosomes was unaffected by the absence of endogenous rapsyn (Fig. 7B), suggesting that the absence of rapsyn specifically affected the clustering of lysosomes. In *Rapsn*$^{-/-}$ myoblasts, lysosomes were scattered into an area (555±50 μm^2, mean±s.e.m., n=25) nearly double of that of *Rapsn*$^{+/+}$ myoblasts [298±28 μm^2, mean±s.e.m., n=18) and C2C12 myoblasts (284±12 μm^2, mean±s.e.m., n=55) (Fig. 7C). The compactness index of lysosomes in *Rapsn*$^{-/-}$ myoblasts (0.014±0.001, mean±s.e.m., n=22) was ∼42% that of *Rapsn*$^{+/+}$ (0.034±0.004, mean±s.e.m., n=11, P<0.0001) and only 23% of that of C2C12 myoblasts (0.062±0.005, mean±s.e.m., n=51, P<0.0001] (Fig. 7D). These results indicate that endogenous rapsyn is required for the positioning and clustering of lysosomes in the juxtanuclear region. When the mobility of lysosomes was examined, we found that the movement of lysosomes was significantly increased in *Rapsn*$^{-/-}$ myoblasts (mean velocity is 0.15 μm/s, see Movie 4) compared to C2C12 myoblasts (Movie 2).

Wild-type rapsyn, but not rapsyn lacking myristoylation, rescues the lysosomal defect in *Rapsn*$^{-/-}$ myoblasts

To examine whether the abnormal lysosomal distribution phenotype in *Rapsn*$^{-/-}$ cells can be rescued by exogenous rapsyn, we transfected *Rapsn*$^{-/-}$ myoblasts with rapsyn–EGFP and compared the lysosomal distribution to control *Rapsn*$^{-/-}$ expressing Lamp1–mCherry only. Indeed, rapsyn–EGFP restored completely the clustering of lysosomes in the cytoplasmic juxtanuclear region of *Rapsn*$^{-/-}$ myoblasts with no scattered lysosomes (Fig. 7E). Quantification of the area occupied by lysosomes in cells expressing wild-type rapsyn–EGFP showed it was significantly reduced (112±14 μm^2, mean±s.e.m., n=12) to ∼20% of the area occupied by lysosomes in control *Rapsn*$^{-/-}$ cells (Fig. 7G). This result suggests that rapsyn is sufficient to induce the clustering of lysosomes. However, the distribution of early endosomes was not affected by over-expression of wild-type rapsyn–EGFP (Fig. 7F), suggesting that rapsyn specifically affected the clustering of lysosomes. When rapsyn lacking the myristoylation site was introduced into *Rapsn*$^{-/-}$ myoblasts, the rescue of lysosome clustering was not observed (Fig. 7E). The area occupied by lysosomes in *Rapsn*$^{-/-}$ myoblasts expressing rapsyn-G2A mutant (752±85 μm^2, mean±s.e.m., n=10) was similar to that of control *Rapsn*$^{-/-}$ myoblasts (555±50 μm^2, mean±s.e.m., n=25) (Fig. 7G). The compactness index of lysosomes of *Rapsn*$^{-/-}$ myoblasts expressing rapsyn G2A-EGFP (0.008±0.001, mean±s.e.m., n=13) was similar to that of control *Rapsn*$^{-/-}$ myoblasts (0.014±0.001, mean±s.e.m., n=29), but only 10% of that of *Rapsn*$^{-/-}$ myoblasts expressing wild-type rapsyn–EGFP (0.16±0.02, mean±s.e.m., n=10) (Fig. 7H). These data suggest that rapsyn is crucial for the clustering and stability of lysosomal organelles.

Rapsyn controls lysosomal exocytosis

Several studies have reported that exocytosis of lysosomes contributes to the resealing of plasma membrane (Miyake and McNeil, 1995; Reddy et al., 2001; Chakrabarti et al., 2003; Andrews et al., 2014). By contrast, rapsyn has also been shown to interact with cytoskeletal proteins (Dobbins et al., 2008). Given the high

Journal of Cell Science

Journal of Cell Science (2015) 128, 3744-3756 doi:10.1242/jcs.172536

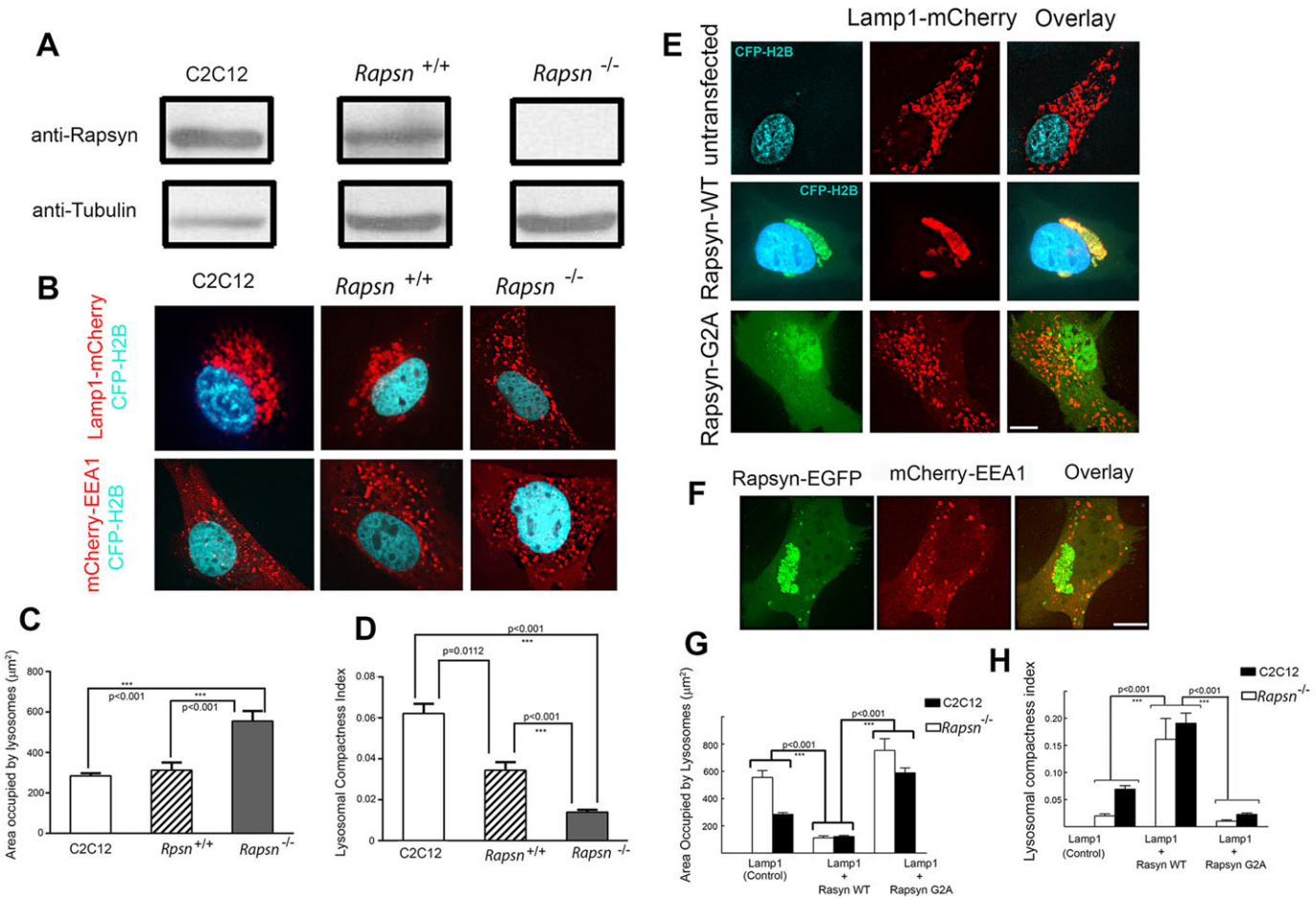

Fig. 7. The clustering of lysosomes in the juxtanuclear region is impaired in rapsyn-deficient myoblasts, whereas exogenous wild-type rapsyn, but not its non-myristoylated form, rescues the lysosome clustering phenotype. (A) Lysates from C2C12, *Rapsn*$^{+/+}$ or *Rapsn*$^{-/-}$ myoblasts were blotted for endogenous rapsyn using a rabbit monoclonal anti-rapsyn antibody or mouse anti-tubulin for loading control. Endogenous rapsyn was detected in C2C12 myoblasts and *Rapsn*$^{+/+}$ myoblasts but not in *Rapsn*$^{-/-}$ myoblasts. (B) Confocal images of live myoblasts expressing CFP–H2B (to label nuclei) and either Lamp1–mCherry or mCherry–EEA1. The top panel shows representative images of C2C12, *Rapsn*$^{+/+}$ or *Rapsn*$^{-/-}$ myoblasts transfected with lysosomal marker Lamp1–mCherry and CFP–H2B. Although lysosomes are distributed in the juxtanuclear region of C2C12 and *Rapsn*$^{+/+}$ myoblasts, they are instead scattered through the entire cytosol in *Rapsn*$^{-/-}$ myoblasts. The bottom panel shows cells expressing EEA1–mCherry and CFP–H2B. Note that the localization of endosomes is not affected by the loss of endogenous rapsyn as a similar distribution of EEA1 was observed in C2C12, *Rapsn*$^{+/+}$ and *Rapsn*$^{-/-}$ myoblasts, indicating that rapsyn selectively affects the lysosomes clustering. (C) Quantification of the area occupied by lysosomes showing a 2-fold increase in the mean area in *Rapsn*$^{-/-}$ compared to either *Rapsn*$^{+/+}$ or C2C12 myoblasts. $P<0.001$. Results are mean±s.e.m. (D) Graph showing the quantification of lysosomal compactness index. Note that the mean compactness index in *Rapsn*$^{-/-}$ is reduced 2.6 times compared to *Rapsn*$^{+/+}$ and 4.6 times compared to C2C12 myoblasts. The *P* values were calculated using Bonferroni test. Results are mean±s.e.m. (E) Representative images of *Rapsn*$^{-/-}$ myoblasts expressing CFP–H2B (to label nuclei) and Lamp1–mCherry without (top panel), or with wild-type rapsyn–EGFP (middle panel), or Lamp1–mCherry and rapsynG2A–EGFP (lower panel). Note that the scattering of the lysosomes in the absence of rapsyn (top panel) was completely rescued in the presence of exogenous wild-type rapsyn–EGFP as the lysosomes clustered back into the juxtanuclear region. In contrast, expression of rapsynG2A–EGFP was unable to reverse the lysosome scattering defect of *Rapsn*$^{-/-}$ myoblasts and the lysosomes remained scattered throughout the cytoplasm (lower panel). (F) Representative images of cells showing that the scattered distribution of early endosomes was not affected by overexpression of wild-type rapsyn–EGFP. Scale bars: 10 μm. (G) Quantification of the area occupied by lysosomes in *Rapsn*$^{-/-}$ myoblasts transfected with Lamp1–mCherry only (untransfected control) or with wild-type rapsyn–EGFP or rapsynG2A–EGFP. Note that in the presence of wild-type rapsyn–EGFP, the area occupied by lysosomes is 5-fold lower than in the absence of rapsyn–EGFP and 6.7-fold lower than in the presence of rapsynG2A–EGFP. For comparison, corresponding data for C2C12 myoblasts are shown side by side. Note that wild-type rapsyn–EGFP rescues the lysosome clustering to the level observed in C2C12 myoblasts. Results are mean±s.e.m. (H) Graph summarizing the quantification of the lysosome compactness index. Note that the index of lysosomal compactness is significantly increased in *Rapsn*$^{-/-}$ myoblasts transfected with exogenous wild-type rapsyn–EGFP (0.16±0.02, mean±s.e.m., $n=10$) compared to control *Rapsn*$^{-/-}$ myoblasts (0.014±0.001, mean±s.e.m., $n=29$) or *Rapsn*$^{-/-}$ myoblasts transfected with rapsynG2A–EGFP (0.008±0.001, mean±s.e.m., $n=13$).

mobility of lysosomes in rapsyn-deficient myoblasts, it is therefore possible that the absence of endogenous rapsyn might have an effect on lysosomal exocytosis and consequently the maintenance of the integrity of the plasma membrane. To examine this idea, we first asked whether the high mobility of lysosomes in *Rapsn*$^{-/-}$ myoblast cells is associated with extracellular release of lysosomal enzymes, a hallmark of lysosomal exocytosis. Analysis of specific lysosomal enzyme β-N-acetylglucoseaminidase (NAG) in culture medium (Fig. 8A) showed that the secretion of this enzyme was significantly increased in rapsyn-deficient (37.78±1.02%, mean±s.e.m., $n=3$) compared to C2C12 myoblasts (17.0±1.48%, mean±s.e.m., $n=3$) ($P<0.0003$). A similar increase in the secretion of lysosomal acid phosphatase was obtained in rapsyn-deficient myoblasts (13.2±0.888%, mean±s.e.m., $n=3$) compared to C2C12 myoblasts

Journal of Cell Science (2015) 128, 3744-3756 doi:10.1242/jcs.172536

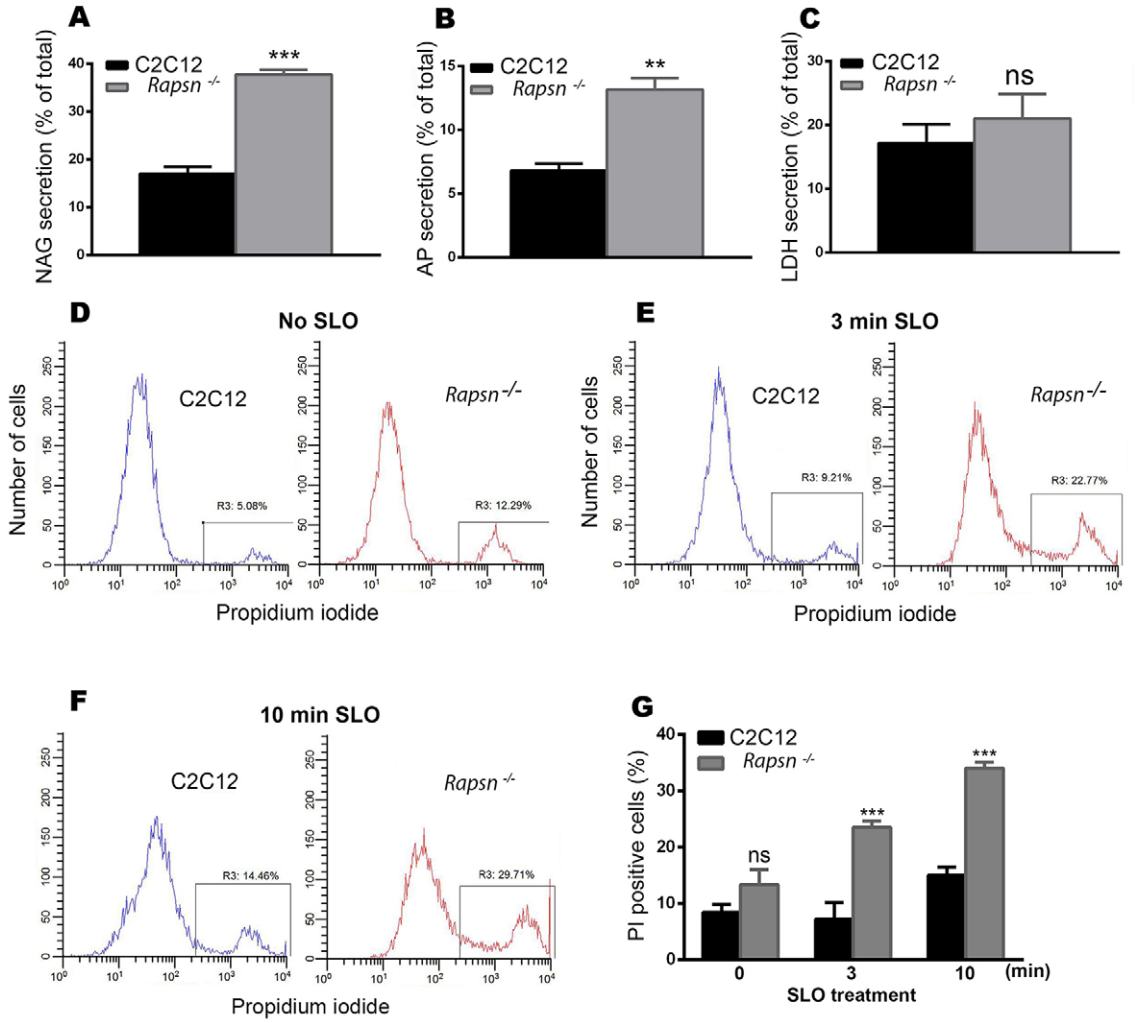

Fig. 8. Lysosomal exocytosis was significantly increased in *Rapsn*$^{-/-}$ myoblasts. Graphs showing lysosomal enzyme activities. (A) β-N-acetylglucoseaminidase (NAG), (B) acid phosphatase (AP) and (C) Lactate dehydrogenase (LDH). Note that both lysosomal enzymes were significantly increased in rapsyn-deficient myoblasts compared to C2C12 myoblasts. Results are mean±s.e.m. (D–F) Representative histograms obtained by FACS analysis of propidium iodide staining of live cells: (D) non-treated C2C12 myoblasts (left) and *Rapsn*$^{-/-}$ (right) myoblasts; (E) treated (permeabilized) myoblasts exposed to 500 µg/ml of bacterial toxin streptolysin-O (SLO) for 3 min or (F) 10 min. In each histogram, the left peak corresponds to intact (propidium iodide negative) cells and the right peak corresponds to propidium-iodide-positive cells. Note that untreated *Rapsn*$^{-/-}$ myoblasts show a higher basal uptake of propidium iodide than C2C12 cells, indicative of plasma membrane damage. This difference in propidium iodide uptake becomes larger as cells are challenged with SLO for 3 min (E) or 10 min (F), indicating that in the absence of rapsyn, plasma membrane is more vulnerable to damage. (G) Quantification of FACS data (as shown in D,E, and F), which is reported as percentage of propidium-iodide-positive *Rapsn*$^{-/-}$ and C2C12 myoblasts that were either untreated (0 min) or treated with SLO for the indicated periods of time. The data represent mean±s.e.m. from three independent experiments.

(6.80±0.551%, mean±s.e.m., n=3) (P<0.0037) (Fig. 8B). This increase in the secretion of lysosomal enzymes was not due to cell death as there was no significant difference in the extracellular release of cytosolic lactate dehydrogenase (LDH), whose release is widely used as marker of cell death, between *Rapsn*$^{-/-}$ (21.0±3.87%, mean±s.e.m., n=3) and C2C12 (17.2±2.96%, mean±s.e.m., n=3) myoblasts (P<0.4756) (Fig. 8C). In COS cells overexpressing dominant-negative rapsynG2A–EGFP (a mutant that induces the scattering of the lysosomes), the acid phosphatase release (7.60±0.404%, mean±s.e.m., n=3) was significantly increased compared to 5.93±0.318% (mean±s.e.m., n=3) for control COS cells (P<0.0316), whereas it was slightly decreased in cells overexpressing wild-type rapsyn–EGFP (4.77±0.233%, mean±s.e.m., n=3) (P<0.0416); this is likely due to low transfection efficiency. However, the difference in acid phosphatase release was more noticeable in rapsynG2A-expressing COS cells (7.60±0.404%, mean±s.e.m., n=3) than wild type (4.77±0.233%, mean±s.e.m., n=3) (P<0.0037). There was, however, no differences in cell viability, as measured by LDH release, between cells transfected with either G2A (38.5±0.786%, mean±s.e.m., n=3, P<0.6402) or wild-type (42.8±1.48%, mean±s.e.m., n=3, P<0.2112) rapsyn–EGFP and control COS cells (36.5±4.02%, mean±s.e.m., n=3), thus excluding any effect of cell death (Fig. S2B). These results suggest that the scattering and high mobility of lysosomes in *Rapsn*$^{-/-}$ cells correlate with increased release of lysosomal enzymes, indicative of enhanced lysosomal exocytosis. However, it appears that the acidic pH of lysosomes is unaffected by gain- and loss-of-function of rapsyn (data not shown).

Next, we asked whether this increase in lysosomal exocytosis is associated with a possible defect in the plasma membrane of rapsyn-deficient cells, given that lysosomal exocytosis is known to contribute to plasma membrane resealing (Miyake and McNeil, 1995; Reddy et al., 2001; Chakrabarti et al., 2003; Andrews et al., 2014). To test this, live *Rapsn*$^{-/-}$ and C2C12 myoblasts were stained

Journal of Cell Science (2015) 128, 3744-3756 doi:10.1242/jcs.172536

with propidium iodide and the permeability of the plasma membrane was analyzed using a fluorescence-activated cell sorting (FACS)-based fluorescent propidium iodide uptake assay (Tam et al., 2010). We found that 13.4±2.6% (mean±s.e.m.) of *Rapsn*$^{-/-}$ myoblasts were propidium-iodide-positive compared to 8.4±1.4% (mean±s.e.m.) of propidium-iodide-positive C2C12 cells (Fig. 8D,G), indicating that the plasma membrane of *Rapsn*$^{-/-}$ cells was compromised. To confirm that the plasma membrane is more prone to damage in the absence of endogenous rapsyn, we challenged *Rapsn*$^{-/-}$ and C2C12 cells with the bacterial pore-forming toxin streptolysine-O (SLO) (Rodríguez et al., 1997) for increasing periods of time and monitored the permeability of their plasma membrane by FACS analysis. After 3 min of SLO treatment, 23.5±2.0% (mean±s.e.m., n=3) of *Rapsn*$^{-/-}$ myoblasts were propidium-iodide-positive compared to only 10.2±0.7% (mean±s.e.m., n=3) for C2C12 cells (Fig. 8E,G). The proportion of PI positive *Rapsn*$^{-/-}$ cells increased to 34±1.1% (s.e.m., N=3) after 10 min of SLO treatment compared to only 15±1.5% (mean±s.e.m., n=3) for C2C12 cells (Fig. 8F,G). These results indicate that the plasma membrane is more prone to damage in *Rapsn*$^{-/-}$ myoblasts. Taken together, our findings indicate that the plasma membrane in rapsyn-deficient cells is susceptible to damage and that the observed increase in lysosomal exocytosis might contribute to the resealing of the plasma membrane to compensate for the lack of endogenous rapsyn.

DISCUSSION

In the current work, we provide evidence for a new function of rapsyn in non-muscle cell types and undifferentiated myoblasts. In addition to its classical role in the aggregation of nicotinic acetylcholine receptor and the formation of neuromuscular junction (Gautam et al., 1995; Sanes and Lichtman, 2001), we demonstrate that rapsyn specifically clusters lysosomes in the juxtanuclear region. This is suggested by (1) the specific localization of rapsyn on lysosomes, precisely at junctions between vacuolin-1-enlarged lysosomes; (2) the dramatic increase in the density of lysosome clusters in the juxtanuclear region of cells overexpressing rapsyn; (3) the fact that disruption of the myristoylation site or deletion of either the coiled-coil or RING-H2 domain not only prevented rapsyn from being targeted to lysosomes but also induced the declustering of lysosomes from the juxtanuclear region; (4) the failure of lysosomes to cluster in rapsyn-deficient myoblasts, wherein they are scattered throughout the cytoplasm; (5) the increase in lysosome mobility in the absence of endogenous rapsyn or in myoblasts transfected with mutated forms of rapsyn; and finally, (6) the complete rescue of lysosomal clustering by exogenous expression of rapsyn–GFP in rapsyn-deficient myoblasts. Taken together, these results provide evidence that rapsyn serves as a clustering agent of lysosomes at the juxtanuclear region.

Based on previous and current studies, we propose that rapsyn performs two functions: (1) in differentiated muscles, rapsyn functions as a clustering agent for AChRs and neuromuscular synapse formation, and (2) in non-muscle cells and undifferentiated myoblasts, which do not express AChRs, rapsyn plays a role in the clustering of lysosomes in the juxtanuclear region. It should be noted that the expression of rapsyn is similar between non-differentiated and differentiated muscle cells, whereas AChR production is undetectable in undifferentiated muscle cells but shows a more than 100-fold increase in differentiated myotubes (Frail et al., 1989). Thus, we propose that rapsyn serves as a clustering molecule for lysosomes in myoblast cells, and when myotubes are differentiated and gene expression of receptors is upregulated, it serves as a clustering agent for AChRs.

The present study shows that rapsyn localizes specifically to lysosomes, as no colocalization between rapsyn and other intracellular organelles was observed, and that it is more precisely concentrated at the junctions between vacuolin-1-enlarged lysosomal vacuoles. In contrast to previous studies, which showed that rapsyn partially overlaps with the trans-Golgi network of COS cells (Marchand et al., 2002), we did not detect colocalization of rapsyn–EGFP with either ManII–mCherry or anti-GM130 antibody staining. Although the source of the discrepancy between the current study and previous ones remains unclear, one potential explanation is that in previous studies rapsyn–GFP was coexpressed with receptor subunits, which might have had an effect on rapsyn targeting to intracellular organelles. It is also worth noting that in the previous studies a lysosomal marker was not used to examine the intracellular localization of rapsyn–GFP (Marchand et al., 2002).

The present work shows that the targeting of rapsyn to lysosomes in the juxtanuclear region requires myristoylation of the N-terminal glycine residue, and the coiled-coil and RING-H2 domains (Figs 5 and 6). Disruption of the myristoylation site results in the build-up of nuclear rapsyn (Figs 5 and 6), and deletion of the coiled-coil or RING-H2 domain results in diffuse distribution throughout the cytoplasm (Fig. 6). This indicates that these structural features of rapsyn are necessary for lysosomal targeting and excludes the possibility that rapsyn concentration at junctional sites between lysosomes results from self-association because the TPR domains that mediate self-association (Ramarao et al., 2001) remained intact in these mutants. Interestingly, the introduction of rapsyn mutants into undifferentiated C2C12 myoblasts induced the declustering of lysosomes from the juxtanuclear region. This suggests that these mutants interfere with the function of endogenous rapsyn and behave as a dominant negative. It is conceivable that exogenous rapsyn–EGFP mutants prevent endogenous rapsyn from being targeted to lysosomes by association through TPR domains, leading to the declustering of lysosomes. Consistent with these findings, the juxtanuclear localization of lysosomes in rapsyn-deficient myoblasts was dramatically affected, as no lysosomal clusters were formed. Instead, lysosomes were scattered throughout the cytoplasm. The defect of lysosomal clustering in rapsyn-deficient myoblasts can be completely rescued by expressing wild-type, but not mutated forms of, rapsyn–EGFP. Collectively, these data highlight the crucial role of rapsyn in the clustering of lysosomes to their proper compartment.

How could rapsyn specifically induce the clustering of lysosomes? Given that rapsyn is concentrated at junctional contacts between lysosomes, it is plausible that it might serve as a molecular link between lysosomes through its myristoylation site, independently of the involvement of lysosomal membrane proteins, given that rapsyn is capable of self-association (Ramarao et al., 2001). Alternatively, it is possible that rapsyn might promote the fusion of lysosomes by acting as a molecular link between SNARE complexes that are pre-assembled on each lysosomal membrane or by inducing their clustering at junctions. Consistent with this, rapsyn colocalizes with VAMP7 (Fig. S2C). Previous studies have shown that Rab7 is involved in the fusion of lysosomes by binding to the homotypic fusion and protein sorting (HOPS) complex (Wurmser et al., 2000; Abenza et al., 2010, 2012; Ostrowicz et al., 2010; Balderhaar and Ungermann, 2013). Thus, it is possible that rapsyn also promotes the clustering of Rab7 either directly or indirectly through its association with the Rabring 7 effector as implied by its colocalization with Rab7. Of note, Rab7 interacts

Journal of Cell Science (2015) 128, 3744-3756 doi:10.1242/jcs.172536

with its Rabring effector through a RING domain (Mizuno et al., 2003) and given that rapsyn also contains a RING domain, it is plausible that rapsyn might also interact with the Rab7 effector Rabring 7 and that deletion of this domain might be involved in the declustering of lysosomes. It is worth mentioning that not all Rab7 molecules colocalize with rapsyn, as some have also been found in late endosomes (Bucci et al., 2000).

At the neuromuscular junction, microtubules and intermediate filaments have been shown to play important roles in the stability of AChR at the postsynaptic apparatus. Rapsyn, a required protein for AChR clustering, has also been shown to interact with several cytoskeletal proteins that are enriched in the postsynaptic apparatus. This includes ACF7 (a protein of the spectrin superfamily) (Antolik et al., 2007), α-actinin [a scaffolding cytoskeletal protein known to cross-link F-actin that mediates AChR clustering (Dobbins et al., 2008)], plectin 1f (a versatile crosslinker protein that links desmin intermediate filament network to dystrophin glycoprotein complex and rapsyn) (Hijikata et al., 2008; Mihailovska et al., 2014) and PKA (a kinase that is crucial for proper AChR stabilization) (Choi et al., 2012). The linkage of rapsyn with these cytoskeletal components is important for keeping AChR stable at the postsynaptic membrane. It is possible that the interaction of rapsyn with cytoskeletal components might also play a potential role in the coalescence of lysosomes in the juxtanuclear region. Our results indicate that the stickiness of lysosomes to rapsyn is not dependent on microtubules as addition of nocodazole to myoblasts does not cause dispersion of rapsyn and lysosomes, at least on the time scale investigated. However, our results do not exclude the role of kinesins, cytoplasmic dynein and others in the coalescence of rapsyn and lysosomes in the juxtanuclear region. This issue warrants further investigation.

The present experiments show that rapsyn controls the dynamic state and exocytosis of lysosomes. Indeed, in cells deficient in rapsyn or cells transfected with a non-myristoylated rapsyn mutant, both the mobility of lysosomes (Movies 2 and 4) and release of lysosomal enzymes into the extracellular environment (Fig. 8) were increased significantly. Interestingly, our results show that the plasma membrane of rapsyn-deficient myoblasts is susceptible to damage as demonstrated by increased permeability to propidium iodine (Fig. 8). Thus it is possible that the high dynamism of lysosomes and the increase of lysosome exocytosis might constitute a compensatory mechanism for membrane resealing and survival of cells. Consistent with these results, previous report have shown that lysosomal exocytosis plays an important role in the resealing of plasma membrane (Miyake and McNeil, 1995; Reddy et al., 2001; Chakrabarti et al., 2003; Andrews et al., 2014). Along these lines, previous studies have reported that the dynamic state and positioning of lysosomes regulates mTORC1 signaling and autophagosome–lysosome fusion in response to nutrient availability (Korolchuk et al., 2011).

In summary, in addition to the classical role of rapsyn in clustering postsynaptic AChRs and formation of neuromuscular junction, the present study suggests a novel function of rapsyn independent of the presence of AChRs. We propose that rapsyn is essential for the clustering and positioning of lysosomes in the juxtanuclear region.

MATERIALS AND METHODS

Plasmids and reagents

Rapsyn–GFP and CamKIIβm–GFP were kindly provided by Jonathan Cohen (Harvard Medical School, Boston, MA) and Ulrich Bayer (University of Colorado, Denver, CO), respectively. α-syntrophin–GFP, α-dystrobrevin–GFP were generated in our laboratory as described previously (Mouslim et al., 2012). Lamp1–GFP and GFP–EEA1 were generous gifts from Haoxing Xu (University of Michigan, Ann Arbor, MI). ManII–mCherry was a gift from Yanzhuang Wang (University of Michigan). EMTB–3×EGFP was a gift from Ann Miller (University of Michigan). mCherry–EEA1 was generated by swapping GFP from GFP–EEA1 with mCherry using EcoRI and XbaI restriction sites. Rapsyn–EGFP (WT, G2A, ΔRING-H2, ΔCC, and ΔCC-RING-H2) constructs were generated first by cloning a wild-type rapsyn PCR product into the pEGFP-N3 vector using XhoI and HindIII restriction sites and then using it as a template to mutate glycine-2 to alanine or delete the coiled-coil, RING-H2 or both domains. Rapsyn–mCherry was generated by replacing EGFP from rapsyn–EGFP with mCherry using the BamHI and XbaI restriction sites.

Vacuolin-1 (CAS 351986) was purchased from Calbiochem and dissolved in DMSO at 20 µg/µl (3.5 mM). Cells were treated at 10 ng/µl (1.75 µM) for ∼3 h prior to live imaging. Rat anti-Lamp1 (1D4B) and mouse anti-tubulin (AA3.4) antibodies were purchased from Developmental Studies Hybridoma Bank (University of Iowa). Rabbit anti-rapsyn (EPR9759), rabbit anti-EEA1 (ab 2900) and rabbit anti-GM130 (ab 53649) antibodies were purchased from Abcam (Cambridge, MA). Rabbit anti-GFP (A6455) was purchased from Invitrogen. Mouse monoclonal anti-rapsyn (clone 1234, R2029) was purchased from Sigma (St Louis, MO).

Cell culture

C2C12 myoblasts were purchased from American Type Culture Collection (Manassas, VA) and maintained in Dulbecco's Modified Eagle's Medium (DMEM) (11995-065; Gibco, NY) supplemented with 20% fetal bovine serum (FBS) (S11050, Atlanta Biologicals, GA). PC12 neuronal cells (a generous gift from Edward Stuenkel, University of Michigan) were maintained in RPMI (11875-093; Gibco) medium supplemented with 10% horse serum (16050; Gibco) and 2% FBS. Chinese Hamster Ovary (CHO) cells (a generous gift from Yanzhuang Wang; University of Michigan) were maintained in F12K (21127-022; Gibco) medium supplemented with 10% FBS. COS-7, HEK and NIH3T3 cells were purchased from ATCC and maintained in Dulbecco's modified Eagle's medium (DMEM) with 10% FBS.

All cells were grown in the presence of 100 U/ml penicillin and 100 µg/ml streptomycin at 37°C, under a humidified atmosphere and 5% CO_2. Cells were transfected at 80% confluency using Lipofectamine 2000 (1467572; Invitrogen) according to the manufacturer's instructions.

Rapsyn-deficient myoblasts (*Rapsn*$^{-/-}$; clone 11-7) and rapsyn wild-type myoblasts (*Rapsn*$^{+/+}$; clone 12-10) were a generous gift from Lin Mei (Georgia Reagents University, GA). These cells were maintained at 33°C under 5% CO_2 in DMEM supplemented with 20% FBS, 4 U/ml mouse γ-interferon (RKP01580; Reprokine, Israel), 0.5% chicken embryo extract (C3999; US Biological, MA).

Western blots

Cells were grown to 90–100% confluence, washed out with cold PBS and lysed with buffer containing 20 mM HEPES pH 7.8, 150 mM NaCl, 2 mM EDTA, 5 mM NaF, 1% Nonidet P-40, 0.5% sodium deoxycholate, 1 mM phenylmethanesulphonyl fluoride and protease inhibitor cocktail (11 873 580 001; Roche, Germany). Lysates were then cleared by centrifugation for 10 min at 12,000 ***g*** and proteins were separated by SDS-PAGE (10%) and transferred to PVDF membranes. The membranes were bathed in blocking solution (3% dry milk and 0.05% Tween 20) for 1 h and then incubated with rabbit monoclonal anti-rapsyn antibody (1:5000), rabbit anti-GFP antibody (1:5000) or mouse anti-tubulin (1:15,000) antibodies overnight at 4°C. The membranes were then incubated for 1 h with horseradish peroxidase (HRP)-conjugated goat anti-rabbit-IgG (1:10,000) or goat anti-mouse-IgG (1:10,000) antibodies. After extensive washing, the membranes were bathed with SuperSignal West Pico solutions (34077; Thermo Fisher Scientific).

Transfection and live cell imaging with spinning disk confocal microcopy

For live imaging, cells were transfected in 35-mm dishes with glass bottoms (P35G-0-14-C; MatTek, MA). At 24 h after transfection, culture medium

was exchanged with fresh medium and cells were either left untreated or treated with vacuolin-1 at 10 ng/µl for ∼3 h prior to imaging. Cells expressing different constructs (see above) were imaged live using an inverted Andor/Olympus IX81 spinning disk confocal microscope equipped with a heated chamber to maintain the temperature at 37°C during imaging. Confocal images were collected with a 100× oil objective NA 1.49 (Olympus) and an iXon EM-CCD camera (Andor). Image acquisition was controlled and *z*-stacks were generated using MetaMorph Advanced Imaging acquisition software v.7.7.8.0 (Molecular Devices).

Immunocytochemistry

C2C12 myoblasts were transfected with rapsyn–GFP. At 24 h after transfection, cells were fixed with 2% formaldehyde in 10 mM PBS pH 7.4 for 30 min and then permeabilized with 1% Triton X-100. Cells were bathed in a blocking solution containing 5% bovine serum albumin for 1 h and then incubated with primary antibody in blocking solution for 2 h at room temperature at the following dilutions: rat anti-Lamp1 antibody (1:200), rabbit anti-EEA1 antibody (1:200), rabbit anti-GM130 antibody (1:200) and mouse monoclonal anti-rapsyn antibody (1:200). Cells were then rinsed extensively and incubated for 1 h with the following secondary antibodies: Alexa-Fluor-647-conjugated goat anti-rat-IgG (1:500) or Alexa-Fluor-594-conjugated mouse anti-rabbit-IgG (1:500) antibodies.

Quantification of lysosomal compactness

For quantification, we used the 'Analyze Particles' plug-in of ImageJ software (NIH). Before analysis, *z*-stacks were collapsed and binary masks of the projections were generated using an ad hoc threshold (to include all Lamp-1-positive organelles). Lysosome clusters were defined from a Lamp1–mCherry signal as particles with a minimum area of 3 pixels. For each cell, we applied the Analyze Particles function to determine the area and perimeter of the lysosomes, where area is the pixels inside the boundary and perimeter the length of the boundary surrounding the area. The lysosomal compactness index or circularity measures how much a shape is compact compared to a circular shape, which has a maximum compactness. The lysosomal compactness index was then deduced according to the formula $4\pi\times\Sigma\,\text{area}/(\Sigma\,\text{perimeter})^2$ (Bard et al., 2003; Zilberman et al., 2011) in which a maximum compactness index value of 1 is obtained for a fully occupied circle. To determine the area occupied by lysosomes, we used the 'Analyze–Measure' function to directly generate the area occupied by Lamp1–mCherry signal.

Lysosomal enzymatic release assays

Lysosomal enzymatic release assays were performed by using the β-N-acetylglucoseaminidase assay kit (Sigma, CS0780) and acid phosphatase assay kit (Sigma, CS0740). The assays are based on the hydrolysis of 4-nitrophenyl N-acetyl-β-D-glucoseaminide or 4-nitrophenyl phosphate substrate by the β-N-acetylglucoseaminidase (NAG) or acid phosphatase, respectively. The enzymatic hydrolysis of the substrates releases p-nitrophenol which can be measured colorimetrically at 405 nm. Enzymatic activities were measured from both medium (released activity) and cell lysate (intracellular activity). The released activity is reported as a percentage of total (released+intracellular) activity.

Lactate dehydrogenase activity

Lactate dehydrogenase activity was measured using the LDH cytotoxicity assay kit from Abcam (ab65393). Activities were measured in both medium and cell lysate and released activity is reported as a percentage of total activity.

FACS analysis

Confluent C2C12 or *Rapsn*$^{-/-}$ cells were either not treated or treated with 500 ng/ml of streptolysin-O for increasing period of time. Cells were then washed, trypsinized and transferred to new tubes. After centrifugation, cells were resuspended in PBS buffer containing propidium iodide (2 µg/ml) and stained for 10 min before an extra PBS wash and immediately analyzed by flow cytometry. Flow cytometry analysis was performed on MACSQuant and data were analyzed using FACSDiva software (BD). At least 10,000 cells were analyzed. For peak positioning controls, we used non-propidium-iodide-stained (propidium iodide negative) cells and Triton-X-100-treated (propidium iodide positive) cells.

Statistical analysis

Data were analyzed using GraphPad Prism Software. Data are shown as means±s.e.m. Quantitative comparisons of numerical datasets were tested for statistical significance by using Student's *t*-test.

Acknowledgements

We thank Richard Hume, Orie Shafer (University of Michigan) and Hans Rudolf Brenner (University of Basel, Switzerland) for critical comments on the manuscript. We also thank Akaaboune laboratory members (Derick Moen, Paula Da Silva Frost, Isabel Martinez-Pena y Valenzuela and Marcelo Pires-Oliveira) for technical assistance and comments on the manuscript.

Competing interests

The authors declare no competing or financial interests.

Author contributions

M. Aittaleb and P.-J.C. performed the experiments. M. Aittaleb and M. Akaaboune analyzed data and wrote the manuscript.

Funding

This work was supported by the National Institutes of Health [grant number NS-047332 and NS-082615 to M.A.]. Deposited in PMC for release after 12 months.

Supplementary information

Supplementary information available online at
http://jcs.biologists.org/lookup/suppl/doi:10.1242/jcs.172536/-/DC1

References

Abenza, J. F., Galindo, A., Pantazopoulou, A., Gil, C., de los Rios, V. and Penalva, M. A. (2010). Aspergillus RabBRab5 integrates acquisition of degradative identity with the long distance movement of early endosomes. *Mol. Biol. Cell* **21**, 2756-2769.

Abenza, J. F., Galindo, A., Pinar, M., Pantazopoulou, A., de los Rios, V. and Penalva, M. A. (2012). Endosomal maturation by Rab conversion in Aspergillus nidulans is coupled to dynein-mediated basipetal movement. *Mol. Biol. Cell* **23**, 1889-1901.

Andrews, N. W., Almeida, P. E. and Corrotte, M. (2014). Damage control: cellular mechanisms of plasma membrane repair. *Trends Cell Biol.* **24**, 734-742.

Antolik, C., Catino, D. H., O'Neill, A. M., Resneck, W. G., Ursitti, J. A. and Bloch, R. J. (2007). The actin binding domain of ACF7 binds directly to the tetratricopeptide repeat domains of rapsyn. *Neuroscience* **145**, 56-65.

Balderhaar, H. J. k. and Ungermann, C. (2013). CORVET and HOPS tethering complexes - coordinators of endosome and lysosome fusion. *J. Cell Sci.* **126**, 1307-1316.

Bard, F., Mazelin, L., Pechoux-Longin, C., Malhotra, V. and Jurdic, P. (2003). Src regulates Golgi structure and KDEL receptor-dependent retrograde transport to the endoplasmic reticulum. *J. Biol. Chem.* **278**, 46601-46606.

Bartoli, M., Ramarao, M. K. and Cohen, J. B. (2001). Interactions of the rapsyn RING-H2 domain with dystroglycan. *J. Biol. Chem.* **276**, 24911-24917.

Bucci, C., Thomsen, P., Nicoziani, P., McCarthy, J. and van Deurs, B. (2000). Rab7: a key to lysosome biogenesis. *Mol. Biol. Cell* **11**, 467-480.

Carr, C., Tyler, A. N. and Cohen, J. B. (1989). Myristic acid is the NH2-terminal blocking group of the 43-kDa protein of Torpedo nicotinic post-synaptic membranes. *FEBS Lett.* **243**, 65-69.

Chakrabarti, S., Kobayashi, K. S., Flavell, R. A., Marks, C. B., Miyake, K., Liston, D. R., Fowler, K. T., Gorelick, F. S. and Andrews, N. W. (2003). Impaired membrane resealing and autoimmune myositis in synaptotagmin VII-deficient mice. *J. Cell Biol.* **162**, 543-549.

Chen, J. W., Murphy, T. L., Willingham, M. C., Pastan, I. and August, J. T. (1985). Identification of two lysosomal membrane glycoproteins. *J. Cell Biol.* **101**, 85-95.

Chen, J. W., Chen, G. L., D'Souza, M. P., Murphy, T. L. and August, J. T. (1986). Lysosomal membrane glycoproteins: properties of LAMP-1 and LAMP-2. *Biochem. Soc. Symp.* **51**, 97-112.

Choi, K.-R., Berrera, M., Reischl, M., Strack, S., Albrizio, M., Roder, I. V., Wagner, A., Petersen, Y., Hafner, M., Zaccolo, M. et al. (2012). Rapsyn mediates subsynaptic anchoring of PKA type I and stabilisation of acetylcholine receptor in vivo. *J. Cell Sci.* **125**, 714-723.

Dobbins, G. C., Luo, S., Yang, Z., Xiong, W. C. and Mei, L. (2008). alpha-Actinin interacts with rapsyn in agrin-stimulated AChR clustering. *Mol. Brain* **1**, 18.

Frail, D. E., Musil, L. S., Buonanno, A. and Merlie, J. P. (1989). Expression of RAPsyn (43K protein) and nicotinic acetylcholine receptor genes is not coordinately regulated in mouse muscle. *Neuron* **2**, 1077-1086.

Froehner, S. C., Gulbrandsen, V., Hyman, C., Jeng, A. Y., Neubig, R. R. and Cohen, J. B. (1981). Immunofluorescence localization at the mammalian neuromuscular junction of the Mr 43,000 protein of Torpedo postsynaptic membranes. *Proc. Natl. Acad. Sci. USA* **78**, 5230-5234.

Fuhrer, C., Gautam, M., Sugiyama, J. E. and Hall, Z. W. (1999). Roles of rapsyn and agrin in interaction of postsynaptic proteins with acetylcholine receptors. *J. Neurosci.* **19**, 6405-6416.

Gautam, M., Noakes, P. G., Mudd, J., Nichol, M., Chu, G. C., Sanes, J. R. and Merlie, J. P. (1995). Failure of postsynaptic specialization to develop at neuromuscular-junctions of rapsyn-deficient mice. *Nature* **377**, 232-236.

Granger, E., McNee, G., Allan, V. and Woodman, P. (2014). The role of the cytoskeleton and molecular motors in endosomal dynamics. *Semin. Cell Dev. Biol.* **31**, 20-29.

Hijikata, T., Nakamura, A., Isokawa, K., Imamura, M., Yuasa, K., Ishikawa, R., Kohama, K., Takeda, S. and Yorifuji, H. (2008). Plectin 1 links intermediate filaments to costameric sarcolemma through beta-synemin, alpha-dystrobrevin and actin. *J. Cell Sci.* **121**, 2062-2074.

Huynh, C. and Andrews, N. W. (2005). The small chemical vacuolin-1 alters the morphology of lysosomes without inhibiting Ca2+-regulated exocytosis. *EMBO. Rep.* **6**, 843-847.

Kong, X. C., Barzaghi, P. and Ruegg, M. A. (2004). Inhibition of synapse assembly in mammalian muscle in vivo by RNA interference. *EMBO. Rep.* **5**, 183-188.

Korolchuk, V. I., Saiki, S., Lichtenberg, M., Siddiqi, F. H., Roberts, E. A., Imarisio, S., Jahreiss, L., Sarkar, S., Futter, M., Menzies, F. M. et al. (2011). Lysosomal positioning coordinates cellular nutrient responses. *Nat. Cell Biol.* **13**, 453-460.

Marchand, S., Devillers-Thiery, A., Pons, S., Changeux, J. P. and Cartaud, J. (2002). Rapsyn escorts the nicotinic acetylcholine receptor along the exocytic pathway via association with lipid rafts. *J. Neurosci.* **22**, 8891-8901.

Martínez-Martínez, P., Phernambucq, M., Steinbusch, L., Schaeffer, L., Berrih-Aknin, S., Duimel, H., Frederik, P., Molenaar, P., De Baets, M. H. and Losen, M. (2009). Silencing rapsyn in vivo decreases acetylcholine receptors and augments sodium channels and secondary postsynaptic membrane folding. *Neurobiol. Dis.* **35**, 14-23.

Maselli, R. A., Dunne, V., Pascual-Pascual, S. I., Bowe, C., Agius, M., Frank, R. and Wollmann, R. L. (2003). Rapsyn mutations in myasthenic syndrome due to impaired receptor clustering. *Muscle Nerve* **28**, 293-301.

Matteoni, R. and Kreis, T. E. (1987). Translocation and clustering of endosomes and lysosomes depends on microtubules. *J. Cell Biol.* **105**, 1253-1265.

Mihailovska, E., Raith, M., Valencia, R. G., Fischer, I., Banchaabouchi, M. A., Herbst, R. and Wiche, G. (2014). Neuromuscular synapse integrity requires linkage of acetylcholine receptors to postsynaptic intermediate filament networks via rapsyn-plectin 1f complexes. *Mol. Biol. Cell.* **25**, 4130-4149.

Miller, A. L. and Bement, W. M. (2009). Regulation of cytokinesis by Rho GTPase flux. *Nat. Cell Biol.* **11**, 71-77.

Miyake, K. and McNeil, P. L. (1995). Vesicle accumulation and exocytosis at sites of plasma membrane disruption. *J. Cell Biol.* **131**, 1737-1745.

Mizuno, K., Kitamura, A. and Sasaki, T. (2003). Rabring7, a novel Rab7 target protein with a RING finger motif. *Mol. Biol. Cell* **14**, 3741-3752.

Moransard, M., Borges, L. S., Willmann, R., Marangi, P. A., Brenner, H. R., Ferns, M. J. and Fuhrer, C. (2003). Agrin regulates rapsyn interaction with surface acetylcholine receptors, and this underlies cytoskeletal anchoring and clustering. *J. Biol. Chem.* **278**, 7350-7359.

Mouslim, C., Aittaleb, M., Hume, R. I. and Akaaboune, M. (2012). A role for the calmodulin kinase II-related anchoring protein (alphakap) in maintaining the stability of nicotinic acetylcholine receptors. *J. Neurosci.* **32**, 5177-5185.

Musil, L. S., Frail, D. E. and Merlie, J. P. (1989). The mammalian 43-kD acetylcholine receptor-associated protein (RAPsyn) is expressed in some nonmuscle cells. *J. Cell Biol.* **108**, 1833-1840.

Noakes, P. G., Phillips, W. D., Hanley, T. A., Sanes, J. R. and Merlie, J. P. (1993). 43K protein and acetylcholine receptors colocalize during the initial stages of neuromuscular synapse formation in vivo. *Dev. Biol.* **155**, 275-280.

Ohno, K., Engel, A. G., Shen, X.-M., Selcen, D., Brengman, J., Harper, C. M., Tsujino, A. and Milone, M. (2002). Rapsyn mutations in humans cause endplate acetylcholine-receptor deficiency and myasthenic syndrome. *Am. J. Hum. Genet.* **70**, 875-885.

Ostrowicz, C. W., Bröcker, C., Ahnert, F., Nordmann, M., Lachmann, J., Peplowska, K., Perz, A., Auffarth, K., Engelbrecht-Vandré, S. and Ungermann, C. (2010). Defined subunit arrangement and rab interactions are required for functionality of the HOPS tethering complex. *Traffic* **11**, 1334-1346.

Phillips, W. D., Maimone, M. M. and Merlie, J. P. (1991). Mutagenesis of the 43-kD postsynaptic protein defines domains involved in plasma membrane targeting and AChR clustering. *J. Cell Biol.* **115**, 1713-1723.

Ramarao, M. K. and Cohen, J. B. (1998). Mechanism of nicotinic acetylcholine receptor cluster formation by rapsyn. *Proc. Natl. Acad. Sci. USA* **95**, 4007-4012.

Ramarao, M. K., Bianchetta, M. J., Lanken, J. and Cohen, J. B. (2001). Role of rapsyn tetratricopeptide repeat and coiled-coil domains in self-association and nicotinic acetylcholine receptor clustering. *J. Biol. Chem.* **276**, 7475-7483.

Reddy, A., Caler, E. V. and Andrews, N. W. (2001). Plasma membrane repair is mediated by Ca2+-regulated exocytosis of lysosomes. *Cell* **106**, 157-169.

Resh, M. D. (2004). Membrane targeting of lipid modified signal transduction proteins. *Subcell. Biochem.* **37**, 217-232.

Rodríguez, A., Webster, P., Ortego, J. and Andrews, N. W. (1997). Lysosomes behave as Ca2+-regulated exocytic vesicles in fibroblasts and epithelial cells. *J. Cell Biol.* **137**, 93-104.

Sanes, J. R. and Lichtman, J. W. (1999). Development of the vertebrate neuromuscular junction. *Annu. Rev. Neurosci.* **22**, 389-442.

Sanes, J. R. and Lichtman, J. W. (2001). Development: Induction, assembly, maturation and maintenance of a postsynaptic apparatus. *Nat. Rev. Neurosci.* **2**, 791-805.

Shaner, N. C., Campbell, R. E., Steinbach, P. A., Giepmans, B. N. G., Palmer, A. E. and Tsien, R. Y. (2004). Improved monomeric red, orange and yellow fluorescent proteins derived from Discosoma sp. red fluorescent protein. *Nat. Biotechnol.* **22**, 1567-1572.

Stenmark, H., Aasland, R., Toh, B. H. and D'Arrigo, A. (1996). Endosomal localization of the autoantigen EEA1 is mediated by a zinc-binding FYVE finger. *J. Biol. Chem.* **271**, 24048-24054.

Tam, C., Idone, V., Devlin, C., Fernandes, M. C., Flannery, A., He, X., Schuchman, E., Tabas, I. and Andrews, N. W. (2010). Exocytosis of acid sphingomyelinase by wounded cells promotes endocytosis and plasma membrane repair. *J. Cell Biol.* **189**, 1027-1038.

Wurmser, A. E., Sato, T. K. and Emr, S. D. (2000). New component of the vacuolar class C-Vps complex couples nucleotide exchange on the Ypt7 GTPase to SNARE-dependent docking and fusion. *J. Cell Biol.* **151**, 551-562.

Zhang, B., Luo, S., Dong, X.-P., Zhang, X., Liu, C., Luo, Z., Xiong, W.-C. and Mei, L. (2007). Beta-catenin regulates acetylcholine receptor clustering in muscle cells through interaction with rapsyn. *J. Neurosci.* **27**, 3968-3973.

Zilberman, Y., Alieva, N. O., Miserey-Lenkei, S., Lichtenstein, A., Kam, Z., Sabanay, H. and Bershadsky, A. (2011). Involvement of the Rho-mDia1 pathway in the regulation of Golgi complex architecture and dynamics. *Mol. Biol. Cell* **22**, 2900-2911.

Journal of Cell Science

SUPPLEMENTAL FIGURES

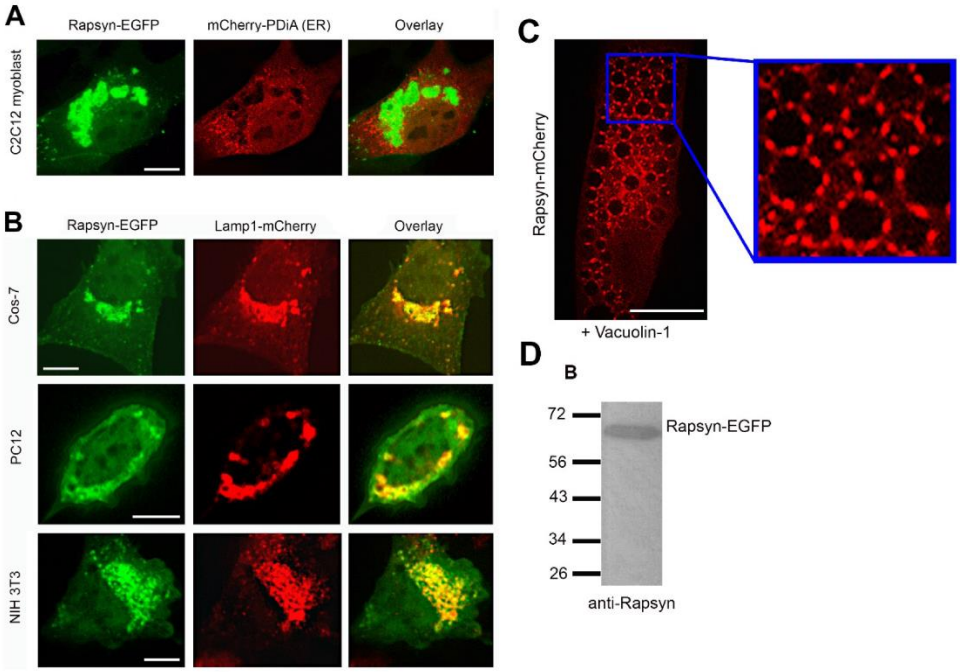

FIGURE S1

A) C2C12 myoblasts were co-transfected with rapsyn-EGFP and endoplasmic reticulum (ER) marker mCherry-PDiA. Transfected cells were imaged live with confocal spinning disk microscope. Representative confocal images showing no overlap between rapsyn-EGFP and mCherry-PDiA, excluding rapsyn targeting to the ER. B) Confocal images of live non-muscle cells co-expressing rapsyn-EGFP and Lamp1-mCherry. As in C2C12 myoblasts, rapsyn-EGFP overlaps with Lamp1-mCherry in COS-7 (top panel), undifferentiated neuronal PC12 (middle panel) and NIH3T3 fibroblasts (lower panel). Scale bar 10μm. C) C2C12 myoblasts were co-transfected with rapsyn-mCherry (mCherry known to resist quenching by the acidic environment of the lysosome lumen) and then treated with vacuolin-1 prior to imaging. Representative confocal image of a live cells showing rapsyn-mCherry concentration at the junctional sites between lysosomal vacuoles and no detectable signal of mCherry inside the lumen. Scale bar 10μm. D) Immunoblot of lysate from C2C12 myoblasts transfected with rapsyn-EGFP and probed with rabbit anti-GFP antibody. No rapsyn proteolytic products were detected.

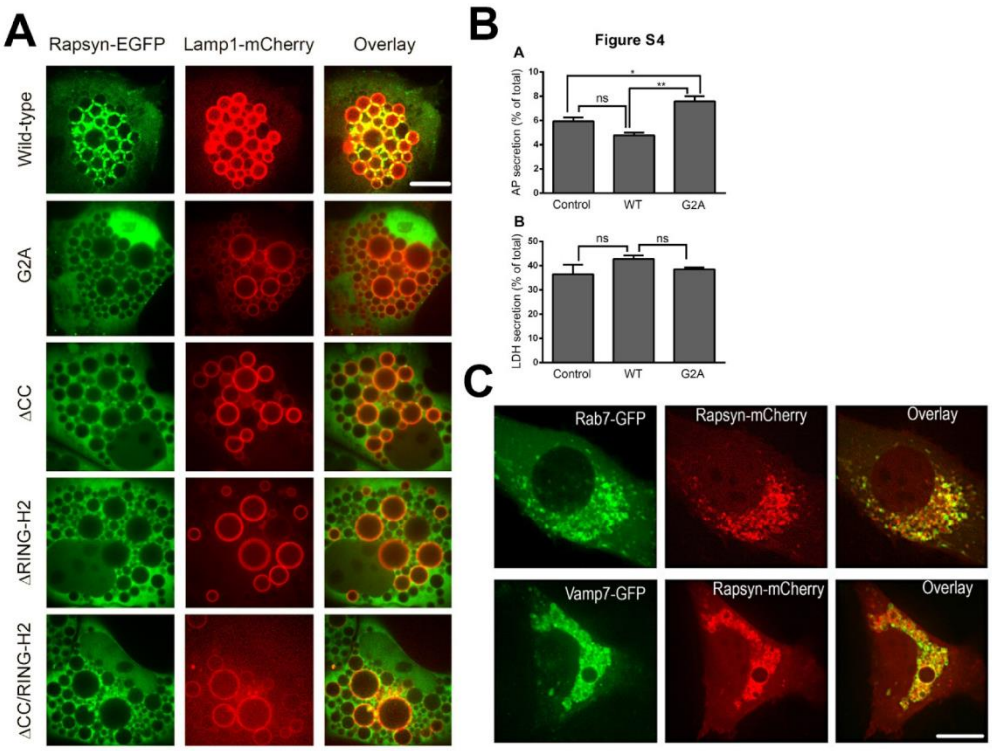

FIGURE S2

A) COS-7 cells were transfected with Lamp1-mCherry and either wild type, G2A, ΔCC, ΔRINGH2 or ΔCC/RINGH2 rapsyn-EGFP constructs. Transfected COS cells were treated with vacuolin-1 prior to live imaging with confocal spinning disk microscopy. Representative confocal images showing that wild type rapsyn-EGFP accumulates in junctional sites between vacuolin-1 enlarged lysosomes in COS cells as was observed in C2C12 myoblasts. G2A mutant however shows prominent accumulation in the nucleus, while ΔCC, ΔRINGH2 and ΔCC/RINGH2 displayed diffuse distribution throughout the cytoplasm. B) Quantification of acid phosphatase (AP) activity released by COS cells either untransfected or transfected with wild-type or G2A rapsyn-EGFP. Released activity is reported as percentage of total activity. B) The corresponding Lactate dehydrogenase (LDH) activities. The data represent mean ±SEM from three independent experiments. C) C2C12 myoblasts were transfected with rapsyn-mCherry and either rab7 (lysosome and late endosome marker) or Vamp7-GFP. Transfected cells were live imaged using spinning disk confocal microscope. Rapsyn-mCherry co-localizes partially with rab7-GFP (top panel) and perfectly with Vamp7-GFP (bottom panel) in the juxtanuclear region of C2C12 myoblasts. Scale bar 10μm.

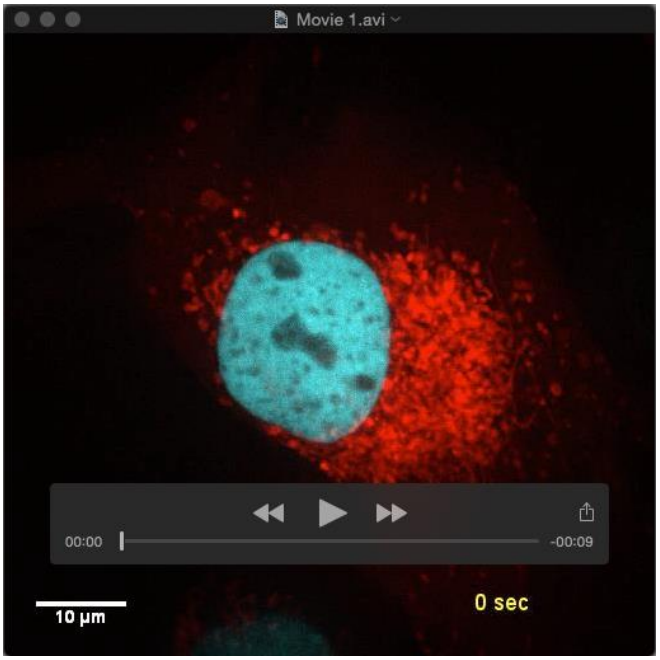

Movie S1

C2C12 control myoblasts were transfected with Lamp1-mCherry and CFP-H2B (to label nuclei) and lysosomal movements were monitored using time lapse imaging. Cells were imaged every 10 seconds. Note that most movements of lysosomes were restricted to the juxtauclear region.

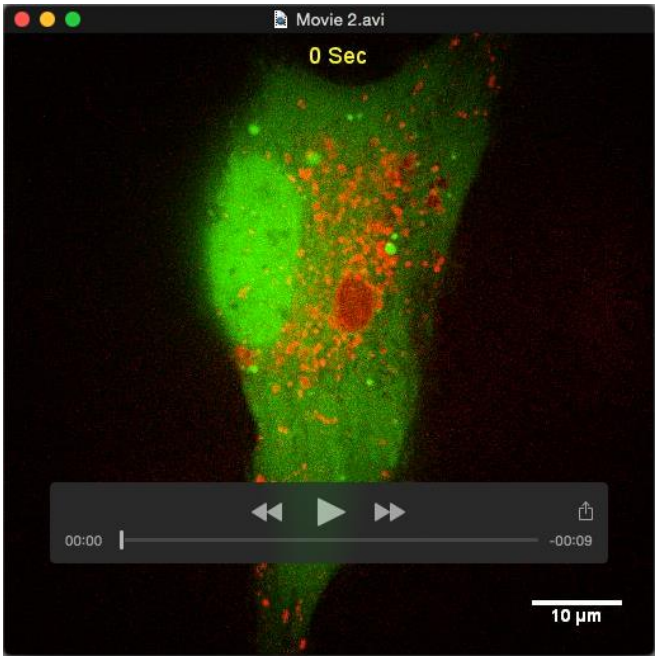

Movie S2

C2C12 myoblasts were co-transfected with Lamp1-mCherry and rapsynG2A-EGFP mutant. Movements of lysosomes in live cells were then monitored by time lapse imaging confocal microscopy. Cells were imaged every 10 seconds. Note that lysosomes are highly mobile in these cells compared to control C2C12 cells.

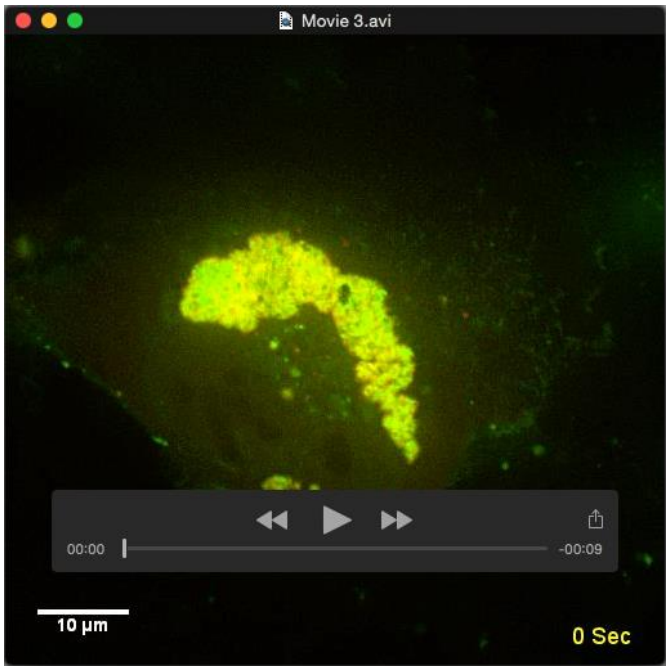

Movie S3

C2C12 myoblasts were co-transfected with Lamp1-mCherry and wild type rapsyn-EGFP constructs. Note that virtually no movement of lysosomes was seen.

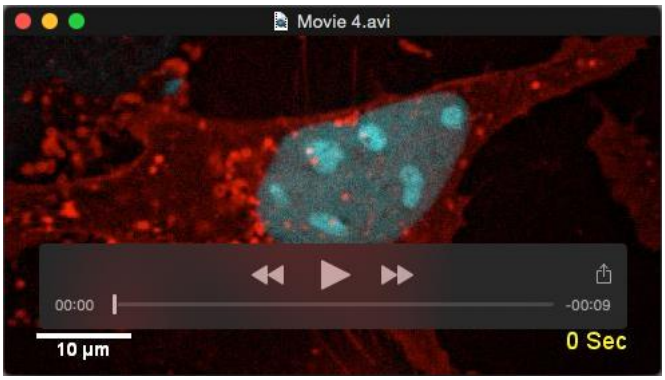

Movie S4

Rapsyn-/- myoblasts were transfected with Lamp1-mCherry and CFP-H2B (to label the nuclei) and movements of lysosomes in live cells were monitored by time lapse imaging. Note that lysosomes are highly mobile in rapsyn-/- compared to control C2C12 cells.